Entropy-satisfying scheme for a hierarchy of dispersive reduced models of free surface flow, Part I

Martin Parisot

Entropy-satisfying scheme for a hierarchy of dispersive reduced models of free surface flow, Part I

Martin Parisot[a]

[a] *Team ANGE (Inria, CEREMA, UPMC, CNRS), 2 rue Simone Iff, CS 42112, 75589 Paris Cedex 12, France and Sorbonne Universités, UPMC Univ. Paris 06, Lab. Jacques-Louis Lions UMR CNRS 7598, 75005 Paris, France*

Abstract

This work is devoted to the numerical resolution in multidimensional framework of a hierarchy of reduced models of the free surface Euler equations, also called water waves equations. The current paper, the first in a series of two, focuses on a hierarchy of monolayer dispersive models, such is the Serre-Green-Naghdi model. A particular attention is given to the dissipation of the mechanical energy at the discrete level, i.e. to design an entropy-satisfying scheme. To illustrate the accuracy and the robustness of the strategy, several numerical experiments are performed. In particular, the strategy is able to deal with dry areas without particular treatment.

Keywords: Free surface flow, Shallow water equations, Dispersive equations, Non-hydrostatic model, Green-Naghdi model, Finite volume method, Entropy satisfying scheme

1. Introduction

The propagation of surface waves is an essential issue for many applications such are harbor planning, tsunami propagation or marine energies. The dynamic of an incompressible, homogeneous, inviscid fluid is governed by the free surface Euler model (E), also called water waves equations. Unfortunately, (E) is too complexe to be simulated at the scale of the applications and some processes such are wet/dry front or breaking wave can be numerically unstable. For geophysical applications, reduced models are largely used because they are simpler and faster to solve numerically. The simpler and the most commonly used for applications nowadays is the non-linear Shallow Water model (SW). The main advantage of (SW) is its mathematical

structure, i.e. hyperbolic, which has led to the design of numerical strategies accurate (good description of shocks and wave celerity [20, 9]) and robust (well-balanced for several steady states [4, 24, 31, 12], entropy-satisfying [21, 39, 35], asymptotic preserving for several regimes [33, 16]). However, it is well-known that (SW) is not a satisfactory model for the propagation of the waves since the dispersive effects are neglected. More precisely, the main assumptions to derive (SW) from (E) are the so-called hydrostatic pressure in the fluid H^p_{yp}) and the homogeneity of the horizontal velocity in the column of water H^u_{yp}). These assumptions are described more precisely in §2.2.

In the past decay, some reduced models were derived from (E) to skirt these assumptions. The Serre-Green-Naghdi model (GN) see [38, 34, 22] takes into account the hydrodynamic pressure, i.e. skirts H^p_{yp}). Several simplified models of it are proposed in the literature and in the following we also consider the non-hydrostatic model (NH) [10] since it is easily classifiable in a hierarchy explained in §2.2. All these models have the particularity to be dispersive and we refer to them as dispersive models in the sequel.

To skirt the second assumption H^u_{yp}), a layerwise discretization with exchange of mass was proposed in [5]. This strategy seems particularly interesting because it preserves the mathematical structure of (SW), at least for a small number of layers, see [1]. Recently, a layerwise version of the dispersive models was proposed [18]. Note that the layerwise discretization is not the only strategy to skirt H^u_{yp}), see [41, 36, 37, 11].

All these models satisfy the conservation or dissipation of the mechanical energy. This property is fondamental in the point of view of mathematics because it is an argument of stability for long time solution and for applications in particular to renewable energies.

The current work is devoted to the numerical resolution of the dispersive models. Several works in the literature deal with the resolution of these models. In [15, 14, 8], a numerical scheme is proposed based a compact form of the equations, i.e. where the only unknowns are the water depth and the horizontal velocity. In spite of a splitting between the shallow water equations (SW) and the dispersive part of the equations, the dispersive step required the discretization of third order derivatives. In addition, the compact form of the equation is not easily adaptable to the layerwise models. In [2, 3], authors propose a developed form of the non-hydrostatic model (NH), where the vertical-averaged vertical velocity is introduced. This new unknowns al-

lowed to add an equation in the hyperbolic step of the previous splitting and limit the dispersive step to a second order elliptic equation. However, the dispersive step is solved by a scheme based on the hydrodynamic pressure and is not easily adaptable to (GN) since in this case the hydrodynamic pressure has two degrees of freedom, see §2.2.

In this paper, the first in a series of two, a new numerical strategy to solve the monolayer dispersive model is proposed. In our knowledge, it is the first numerical scheme for dispersive systems where the the dissipation of the numerical mechanical energy is proven. In addition, the strategy give a framework easily adaptable to (NH) or (GN), and extendable to the layerwise versions. The layerwise numerical schemes are presented in a second paper [32], so we expect to present enough detail to clearly state the numerical method and to present enough test cases to illustrate the behavior of the models.

The current paper is organized as follow. First of all, the free surface Euler model (E) is briefly presented in §2 as well as the hierarchy of reduced models. Then, §3 is devoted to the description of the numerical resolution in multidimensional framework of each models of the hierarchy. Numerical schemes are constructed step by step with the complexity of the models. In §4, a simple treatment of the boundary conditions are presented. Eventually, numerical illustrations in one dimensional framework are presented in §5 which validate the consistance and the robustness of the method.

2. The hierarchy of reduced models

2.1. Incompressible free surface Euler equations (E)

We consider an incompressible, homogeneous, inviscid free surface flow over a topography subjected to the gravity force. The frame (t, x, z) is such that $t \geq 0$ is the time, $x \in \Omega \subset \mathbb{R}^d$ is the horizontal plan coordinate with $d \in \{1, 2\}$, and $z \in \mathbb{R}$ is the vertical coordinate oriented such that z is increasing to the top. The flow is assumed satisfying the free surface incompressible Euler equations with an assumption of mono-valued free surface. More precisely, the fluid is assumed to be contains between a given bottom surface $z = B(t, x)$ and an unknown free surface level $z = \eta(t, x)$ and satisfies for

any $B < z \leq \eta$

$$\begin{cases} \nabla \cdot u & + \partial_z w & = 0 \\ \partial_t u + (u \cdot \nabla) u & + w \partial_z u & = -\nabla p \\ \partial_t w + (u \cdot \nabla) w & + w \partial_z w & = -\partial_z p - g \end{cases} \tag{E}$$

with ∇ and $\nabla\cdot$ are respectively the gradient and the divergence according the x-variable, the horizontal velocity $u(t,x,z) \in \mathbb{R}^d$, the vertical velocity $w(t,x,z) \in \mathbb{R}$, the pressure in the fluid $p(t,x,z) \in \mathbb{R}$ and the gravity acceleration $g \in \mathbb{R}$. At bottom, the no-penetration condition is considered, i.e.

$$\partial_t B + u_{|z=B} \cdot \nabla B = w_{|z=B}$$

and at the free surface, the pressure is given by $p(t,x,\eta(t,x)) = P(t,x)$ and the kinematic condition is considered, i.e.

$$\partial_t \eta + u_{|z=\eta} \cdot \nabla \eta = w_{|z=\eta}.$$

The system of equation have to be completed with an initial condition $\eta(0,x) = \eta^0(x)$, $u(0,x,z) = u^0(x,z)$ and $w(0,x,z) = w^0(x,z)$. Note that the initial condition have to satisfied the compatibility conditions with the divergence free condition and the boundary condition at bottom, i.e.

$$\nabla \cdot u^0 + \partial_z w^0 = 0 \qquad \text{and} \qquad \partial_t B_{|t=0} + u^0_{|z=B} \cdot \nabla B = w^0_{|z=B}.$$

For commodity in the following, we introduce the homogeneous potential

$$\phi(t,x) = gB(t,x) + P(t,x)$$

and the hydrodynamic pressure, also called non-hydrostatic pressure, defined by

$$q(t,x,z) = p(t,x,z) - P(t,x) - g(\eta(t,x) - z).$$

Let us recall the main physical properties of the Euler model (E).

Proposition 1. *Assuming $\eta^0(x) - B(0,x) \geq 0$,*
then the solution of (E) satisfies

1.i) the positivity of the water depth, i.e. $\eta(t,x) - B(t,x) \geq 0$.

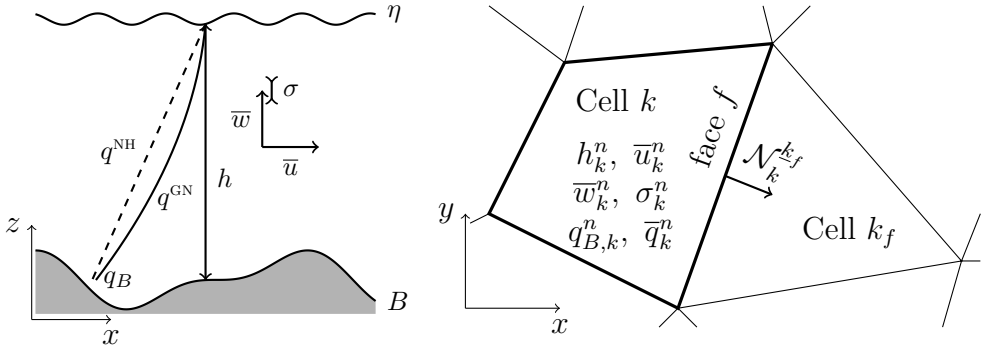

Figure 1: Illustration of the notations. (left) Interpretation of the unknowns in the vertical plan. (right) Finit volume discretization in the horizontal plan.

1.ii) the following mechanical energy balance balance for smooth enough solution

$$\partial_t \left(\mathcal{E}\left(\eta - B\right) + \mathcal{K}^u + \mathcal{K}^w \right) + \nabla \cdot \left(\mathcal{G}^\eta + \mathcal{G}^u + \mathcal{G}^w + \mathcal{G}^q \right) = \left(\eta - B\right) \partial_t \phi + q_{|z=B} \partial_t B$$

with the potential energy

$$\mathcal{E}\left(h\right) = h\left(\phi + g\frac{h}{2}\right), \tag{2.1}$$

the kinetic energy $\mathcal{K}^\psi = \mathcal{K}\left(\eta, \psi\right)$ *with*

$$\mathcal{K}\left(\eta, \psi\right) = \int_B^\eta \frac{1}{2} \left|\psi\right|^2 \mathrm{d}z,$$

and the flux are defined by $\mathcal{G}^\eta = \mathcal{G}\left(\eta, u, P + g\eta\right)$, $\mathcal{G}^u = \mathcal{G}\left(\eta, u, \frac{1}{2}\left\|u\right\|^2\right)$, $\mathcal{G}^w = \mathcal{G}\left(\eta, u, \frac{1}{2}\left|w\right|^2\right)$ *and* $\mathcal{G}^q = \mathcal{G}\left(\eta, u, q\right)$ *with*

$$\mathcal{G}\left(\eta, u, \psi\right) = \int_B^\eta \psi u \, \mathrm{d}z.$$

2.2. Brief description of the monolayer models

In the current section, we present the hierarchy of monolayer reduced models of (E) that are considered in the sequel.

Shallow water model (*SW*)*:* First of all, we present (*SW*) [17] where the hydrodynamic pressure is neglected. The unknowns of (*SW*) are the water depth $h^{\text{SW}}(t,x) \in \mathbb{R}_+$ and the vertical-averaged horizontal velocity $\overline{u}^{\text{SW}}(t,x) \in \mathbb{R}^d$, see Figure 1. More precisely, the unknowns of (*E*) are approximated by

$$\eta \approx B + h^{\text{SW}}\ , \quad u \approx \overline{u}^{\text{SW}}\ , \quad w \approx 0 \quad \text{and} \quad q \approx 0.$$

(*SW*) can be obtained from (*E*) mainly assuming:

H^p_{yp}) the pressure given by the hydrostatic relation $p(t,x,z) \approx P(t,x) + g(\eta(t,x) - z)$.

H^u_{yp}) the horizontal velocity constant in the whole column of water $u(t,x,z) \approx \overline{u}(t,x)$.

A fine derivation from the Navier-Stokes equations is realized in [19]. It is explained that (*SW*) is an approximation of smooth enough solution of the Navier-Stokes equations in $O(\varepsilon)$ where ε is the ratio of the vertical characteristic length over the the horizontal characteristic length. Higher-order approximation can be derived but introduce dissipative terms.

Non-hydrostatic model (*NH*)*:* The simpler considered model approximating the hydrodynamic pressure is (*NH*) [10]. More precisely, the vertical velocity is approximated by its vertical-averaged and leads to a linear approximation of the hydrodynamic pressure. The unknowns of (*NH*) are the water depth $h^{\text{NH}}(t,x) \in \mathbb{R}_+$, the vertical-averaged horizontal velocity $\overline{u}^{\text{NH}}(t,x) \in \mathbb{R}^d$, the vertical-averaged vertical velocity $\overline{w}^{\text{NH}}(t,x) \in \mathbb{R}$ and the hydrodynamic pressure at bottom $q_B^{\text{NH}}(t,x) \in \mathbb{R}$, see Figure 1. More precisely, the unknowns (u,w,q) of (*E*) are approximated in the vertical direction in $\mathbb{P}_0 \times \mathbb{P}_0 \times \mathbb{P}_1$ such that

$$\eta \approx B + h^{\text{NH}}\ , \quad u \approx \overline{u}^{\text{NH}}\ , \quad w \approx \overline{w}^{\text{NH}} \quad \text{and} \quad q \approx \frac{B + h - z}{h} q_B^{\text{NH}}.$$

A fine derivation of (*NH*) from (*E*) is realized in [10].

Serre-Green-Naghdi model (*GN*)*:* To satisfy the divergence free condition, the approximation of the vertical velocity has to be one order higher than the horizontal velocity. In the simple case, the vertical velocity is approximated by a linear function, leads to a quadratic approximation of the hydrodynamic pressure and yields to (*GN*) [38, 34, 22]. The unknowns of (*GN*)

are the water depth $h^{\text{GN}}(t,x) \in \mathbb{R}_+$, the vertical-averaged horizontal velocity $\overline{u}^{\text{GN}}(t,x) \in \mathbb{R}^d$, the vertical-averaged vertical velocity $\overline{w}^{\text{GN}}(t,x) \in \mathbb{R}$, the oriented standard deviation of the vertical velocity $\sigma^{\text{GN}}(t,x) \in \mathbb{R}$, the hydrodynamic pressure at bottom $q_B^{\text{GN}}(t,x) \in \mathbb{R}$ and the vertical-averaged hydrodynamic pressure $\overline{q}^{\text{GN}}(t,x) \in \mathbb{R}$, see Figure 1. More precisely, the unknowns (u,w,q) of (E) are approximated in the vertical direction in $\mathbb{P}_0 \times \mathbb{P}_1 \times \mathbb{P}_2$ such that

$$\eta \approx B + h^{\text{GN}}\ , \quad u \approx \overline{u}^{\text{GN}}\ , \quad w \approx \overline{w}^{\text{GN}} + 2\sqrt{3}\frac{z - B + \frac{h}{2}}{h}\sigma^{\text{GN}}$$
$$\text{and} \quad q \approx \frac{B + h - z}{h} q_B^{\text{GN}} + 3\frac{(z-B)(B+h-z)}{h^2}\left(2\overline{q}^{\text{GN}} - q_B^{\text{GN}}\right).$$

A brief derivation of (GN) is performed in §Appendix A. In particular, it introduce naturally the new formulation on which the discrete scheme in based. Other reconstruction of the unknowns of (E) from the one of the Serre-Green-Naghdi model can be done in particular to satisfy a curl free condition instead of the divergence free condition. A finer derivation of (GN) from (E) and a deeper description is realized in [27]. It explains that (GN) is an approximation of (E) in order of $O(\varepsilon^2)$ and $O(a)$ with a is the ratio between the characteristic wave amplitude and the characteristic water depth.

For readability reason, the exponent SW, NH and GN are dropped out when the model is clear. More precisely, each following subsections are devoted to one model and the unknowns refer to it.

For each model, an entropy-satisfying scheme based on Finite volume discretization is proposed. Let us introduce some notations used in the following. Let $\mathbb{T}$ be a tesselation of $\Omega \subset \mathbb{R}^d$ the horizontal domain, composed of star-shaped control volumes, see Figure 1. We denote by $k \in \mathbb{T}$ a cell, $\mathbb{F}_k$ the set of its faces, $|k|$ its surface area. Furthermore for a face f, its length is denoted $|f|$ and $\underline{k}_f$ is the neighbor cell of k such that $k \cup \underline{k}_f = f$. The space step is defined as the compactness of the star-shaped control volumes, i.e.

$$\delta_k = \begin{cases} \dfrac{|k|}{2} & \text{d=1,} \\ \dfrac{|k|}{\sum_{f\in\mathbb{F}_k}|f|} & \text{d=2.} \end{cases}$$

The unit normal to f outward to k is design by $\mathcal{N}_k^{\underline{k}_f}$. The time is discretized using an adaptative time step, i.e. $t^{n+1} = t^n + \delta_t^n$, with δ_t^n satisfying a CFL

condition described further. The discrete unknowns ψ_k^n is the approximation at time t^n of the mean value of the unknowns ψ in the cell k. For readability, we introduce the discrete time derivative of a variable ψ by

$$\partial_t^{n+1}\psi = \frac{\psi^{n+1} - \psi^n}{\delta_t^n}. \tag{2.2}$$

To describe the schemes, the centered discrete operator $\nabla_k^\delta : (\mathbb{R})^N \to \mathbb{R}^d$ and $\nabla_k^\delta \cdot : \left(\mathbb{R}^d\right)^N \to \mathbb{R}$ are used respectively defined by

$$\nabla_k^\delta \psi = \frac{1}{|k|}\sum_{f\in\mathbb{F}_k} \frac{\psi_{\underline{k}_f} + \psi_k}{2}\mathcal{N}_k^{\underline{k}_f}|f| \qquad \text{and} \qquad \nabla_k^\delta \cdot \psi = \frac{1}{|k|}\sum_{f\in\mathbb{F}_k} \frac{\psi_k + \psi_{\underline{k}_f}}{2}\cdot\mathcal{N}_k^{\underline{k}_f}|f|. \tag{2.3}$$

These discrete operators are clearly consistant respectively with ∇ and $\nabla\cdot$ and are second order.

3. Monolayer models

3.1. Shallow water model (SW)

3.1.1. Governing equations of (SW) and main properties

Let us start the description of the strategy by the well-known shallow water model (*SW*). It reads

$$\begin{aligned} &\partial_t \mathcal{U}^{\text{SW}} + \nabla\cdot F^{\text{SW}}\left(\mathcal{U}^{\text{SW}}\right) = S^{\text{SW}}\left(\mathcal{U}^{\text{SW}}\right) \quad \text{with} \quad \mathcal{U}^{\text{SW}} = \begin{pmatrix} h \\ h\overline{u} \end{pmatrix} \\ &F^{\text{SW}}\left(\mathcal{U}^{\text{SW}}\right) = \begin{pmatrix} h\overline{u} \\ h\overline{u}\otimes\overline{u} + \frac{g}{2}h^2\mathbf{I}_d \end{pmatrix} \quad \text{and} \quad S^{\text{SW}}\left(\mathcal{U}^{\text{SW}}\right) = \begin{pmatrix} 0 \\ -h\nabla\phi \end{pmatrix}. \end{aligned} \tag{SW}$$

The initial condition of (*SW*) is given by $h\left(0,x\right) = h^0\left(x\right)$ and $\overline{u}\left(0,x\right) = \overline{u}^0\left(x\right)$. Let us recall the main physical properties of (*SW*).

Proposition 2. *Assuming $h^0\left(x\right) \geq 0$,*
then the solution of (SW) satisfies

2.i) the positivity of the water depth, i.e. $h\left(t,x\right) \geq 0$.
It is the counterpart of Proposition 1.i).

2.ii) the following mechanical energy balance for smooth enough solution

$$\partial_t\left(\mathcal{E} + \overline{\mathcal{K}}^{\overline{u}}\right) + \nabla\cdot\left(\overline{\mathcal{G}}^{h} + \overline{\mathcal{G}}^{\overline{u}}\right) = h\partial_t\phi$$

with the potential energy $\mathcal{E}(h)$ *defined by* (2.1)*, the kinetic energy owing from the horizontal velocity* $\overline{\mathcal{K}}^{\overline{u}} = \overline{\mathcal{K}}(h, \overline{u})$ *and the flux* $\overline{\mathcal{G}}^{h} = \overline{\mathcal{G}}(h\overline{u}, \phi + gh)$ *and* $\overline{\mathcal{G}}^{u} = \overline{\mathcal{G}}\left(h\overline{u}, \overline{\mathcal{K}}(1, \overline{u})\right)$ *with*

$$\overline{\mathcal{K}}(h, \psi) = \frac{h}{2}\|\psi\|^2 \qquad \text{and} \qquad \overline{\mathcal{G}}(\mathcal{Q}, \psi) = \psi\mathcal{Q} \tag{3.1}$$

More precisely, in case of non-smooth solution, the admissible solution are defined such that the mechanical energy is decreasing, i.e.

$$\partial_t\left(\mathcal{E} + \overline{\mathcal{K}}^{\overline{u}}\right) + \nabla\cdot\left(\overline{\mathcal{G}}^{h} + \overline{\mathcal{G}}^{\overline{u}}\right) \leq h\partial_t\phi.$$

It is the counterpart of Proposition 1.ii).

3.1.2. Entropy-satisfying numerical scheme of (*SW*)

In the past decay, several numerical strategies preserving the main physical properties, in particular Proposition 2, was proposed. In the current work, we briefly recall one of them based on an explicit Finit Volume scheme. For more details, we refer to [9]. The scheme of (*SW*) can be formulate as

$$\mathcal{U}_k^{\mathrm{SW},n+1} = \mathcal{U}_k^{\mathrm{SW},n} - \frac{\delta_t^n}{|k|}\sum_{f\in\mathbb{F}_k}\left(\mathcal{F}_f^{\mathrm{SW},n}\cdot\mathcal{N}_k^{\underline{k}_f} + \mathcal{S}_{f,k}^{\mathrm{SW},n}\right)|f| \tag{SW^δ}$$

with $\mathcal{U}_k^{\mathrm{SW},n} = \left(h_k^n,\ h_k^n\overline{u}_k^n\right)^t$. The numerical flux $\mathcal{F}_f^{\mathrm{SW},n}\cdot\mathcal{N}_k^{\underline{k}_f} = \left(\mathcal{F}_f^{1,n}\cdot\mathcal{N}_k^{\underline{k}_f}, \mathcal{F}_f^{2,n}\cdot\mathcal{N}_k^{\underline{k}_f}\right)^t$ defined by $\mathcal{F}_f^{\mathrm{SW},n}\cdot\mathcal{N}_k^{\underline{k}_f} = \mathcal{F}^{\mathrm{SW}}\left(\mathcal{U}_k^{\mathrm{SW},n}, \phi_k^n; \mathcal{U}_{\underline{k}_f}^{\mathrm{SW},n}, \phi_{\underline{k}_f}^n; \mathcal{N}_k^{\underline{k}_f}\right)$ have to be symmetric and consistant with the mono-dimensional flux

$$F^{\mathrm{SW}}\begin{pmatrix} h \\ h\overline{u}_{\mathcal{N}} \\ h\overline{u}_{\mathcal{T}}\end{pmatrix} = \begin{pmatrix} h\overline{u}_{\mathcal{N}} \\ h\overline{u}_{\mathcal{N}}^2 + \frac{g}{2}h^2 \\ h\overline{u}_{\mathcal{T}}\ \overline{u}_{\mathcal{N}}\end{pmatrix} \qquad \text{with} \qquad \begin{array}{l}\overline{u}_{\mathcal{N}} = \overline{u}\cdot\mathcal{N}_k^{\underline{k}_f} \\ \overline{u}_{\mathcal{T}} = \overline{u}\cdot\mathcal{T}_k^{\underline{k}_f}\end{array}$$

and the source term $\mathcal{S}_{f,k}^{\mathrm{SW},n} = \left(0, \mathcal{S}_{f,k}^{2,n}\right)^t = \mathcal{S}^{\mathrm{SW}}\left(\mathcal{U}_k^{\mathrm{SW},n}, \phi_k^n; \mathcal{U}_{\underline{k}_f}^{\mathrm{SW},n}, \phi_{\underline{k}_f}^n; \mathcal{N}_k^{\underline{k}_f}\right)$ have to be define such that $\frac{1}{|k|}\sum_{f\in\mathbb{F}_k}\mathcal{S}_{f,k}^{2,n}|f|$ is consistant with $-h\nabla\phi$. Several strategies are described in the literature to compute the numerical flux $\mathcal{F}$ and the source term $\mathcal{S}$, see [20, 30, 9, 42].

In the following we ask (SW^δ) to satisfy the following properties under a CFL condition like

$$\lambda\left(\mathcal{U}_k^{\mathrm{SW},n}; \mathcal{U}_{\underline{k}_f}^{\mathrm{SW},n}\right)\delta_t^n \leq \min\left(\delta_k, \delta_{\underline{k}_f}\right) \tag{3.2}$$

with $\lambda\left(\mathcal{U}_L^{\text{SW}};\mathcal{U}_R^{\text{SW}}\right)$ is an upper bound of the speed of propagation, depending on the numerical flux $\mathcal{F}^{\text{SW}}$ used.

Proposition 3. *Under the CFL condition (3.2) and assuming that $h_k^0 \geq 0$, the solution of (SW^δ) satisfies*

3.i) the positivity of the water depth, i.e. $h_k^n \geq 0$.
It is the discrete counterpart of Proposition 2.i).

3.ii) a discrete mechanical energy dissipation. More precisely, there exist two flux $\overline{\mathcal{G}}_\delta^h\left(\mathcal{U}_L^{\text{SW}};\mathcal{U}_R^{\text{SW}}\right)$ and $\overline{\mathcal{G}}_\delta^{\overline{u}}\left(\mathcal{U}_L^{\text{SW}},\mathcal{U}_R^{\text{SW}}\right)$ respectively consistent with $\overline{\mathcal{G}}^h$ and $\overline{\mathcal{G}}^{\overline{u}}$ given in (3.1) such that the discrete mechanical energy satisfies

$$\partial_t^{n+1}\left(\mathcal{E}_k + \overline{\mathcal{K}}_k^{\overline{u}}\right) + \frac{1}{|k|}\sum_{f\in\mathbb{F}_k}\left(\overline{\mathcal{G}}_f^{h,n} + \overline{\mathcal{G}}_f^{\overline{u},n}\right)\cdot\mathcal{N}_k^{\underline{k}_f}\,|f| \leq h_k^n\partial_t^{n+1}\phi_k$$

with $\mathcal{E}_k^n = \mathcal{E}\left(h_k^n\right)$, $\overline{\mathcal{K}}_k^{\overline{u},n} = \overline{\mathcal{K}}\left(h_k^n,\overline{u}_k^n\right)$, $\overline{\mathcal{G}}_f^{h,n} = \overline{\mathcal{G}}_\delta^h\left(\mathcal{U}_k^{\text{SW},n},\mathcal{U}_{\underline{k}_f}^{\text{SW},n}\right)$, $\overline{\mathcal{G}}_f^{\overline{u},n} = \overline{\mathcal{G}}_\delta^{\overline{u}}\left(\mathcal{U}_k^{\text{SW},n},\mathcal{U}_{\underline{k}_f}^{\text{SW},n}\right)$.
It is the discrete counterpart of Proposition 2.ii).

Some numerical strategies ensure the dissipation of the discrete mechanical energy Proposition 3.ii), which act as a mathematical entropy. It is for exemple the case of the Godunov solver [21], the kinetic solver [35], the Suliciu relaxation solver [39] and the CPR scheme [16]. Several others satisfies an approximation of Proposition 3.ii) which is enough in practice. More precisely, the hydrostatic reconstruction [4] ensure the semi-discrete mechanical energy dissipation, i.e. only discrete on space. The kinetic solver with explicit computation of flux [6] satisfies a mechanical energy inequality with a source term proportional to the time step. Some implicit schemes or ImEx schemes ensure the dissipation of the mechanical energy with source term, see for instead [33], and can also be used as well with the numerical strategy of the dissipative models presented in the sequel.

Note that the Proposition 3 is not an exhaustive list of properties that can satisfy a scheme for (SW). Even if translation of these properties at the discrete level is an interesting and challenging issue, it is not the point of the current work. We only highlight that the steady state at rest so-called lake at rest is easily extendable to the dispersive models. More precisely, as it is the case of the positivity of the water depth, the preservation of the lake at rest by the dispersive models will be a trivial consequence of the preservation of the lake at rest by (SW^δ).

3.2. Non-hydrostatic model (NH)

3.2.1. Governing equations of (NH) and main properties

Let us now focus on the second assumption H^p_{yp}). The simpler model in the hierarchy presented in §2.2 is the non-hydrostatic model (NH) that can be formulated as follow

$$\begin{cases} \partial_t h & + \nabla \cdot (h\overline{u}) & = 0 \\ \partial_t (h\overline{u}) & + \nabla \cdot \left(h\overline{u} \otimes \overline{u} + \dfrac{g}{2} h^2 \mathbf{I}_d \right) + h\nabla\phi & = -\nabla \left(h \dfrac{q_B}{2} \right) - q_B \nabla B \\ \partial_t (h\overline{w}) & + \nabla \cdot (h\overline{w}\, \overline{u}) & = q_B \end{cases} \tag{NH.a}$$

with the constrain associated to the Lagrange multiplier q_B reads

$$\overline{w} = \partial_t \left(B + \frac{h}{2} \right) + \overline{u} \cdot \nabla \left(B + \frac{h}{2} \right). \tag{NH.b}$$

An initial condition is required on $h(0,x) = h^0(x)$, $\overline{u}(0,x) = \overline{u}^0(x)$ and $\overline{w}(0,x) = \overline{w}^0(x)$ and have to satisfy the compatibility condition

$$\overline{w}^0 = \partial_t B_{|t=0} + \overline{u}^0 \cdot \nabla B - \frac{h^0}{2} \nabla \cdot \overline{u}^0$$

which in no more than a rewriting of the constrain (NH.b) at the initial time using the conservation of mass. For more detail about (NH), we refer to [10]. Let us first recall the main physical properties of (NH).

Proposition 4. *Assuming that $h^0(x) \geq 0$,*
then the solution of (NH) satisfies

4.i) the positivity of the water depth, i.e. $h(t,x) \geq 0$.
It is the counterpart of Proposition 1.i).

4.ii) the following mechanical energy balance for smooth enough solution

$$\partial_t \left(\mathcal{E} + \overline{\mathcal{K}}^{\overline{u}} + \overline{\mathcal{K}}^{\overline{w}} \right) + \nabla \cdot \left(\overline{\mathcal{G}}^{h} + \overline{\mathcal{G}}^{\overline{u}} + \overline{\mathcal{G}}^{\overline{w}} + \overline{\mathcal{G}}^{q_B} \right) = h\partial_t\phi + q_B \partial_t B$$

with the potential energy $\mathcal{E}(h)$ defined by (2.1), the kinetic energies $\overline{\mathcal{K}}^{\psi} = \overline{\mathcal{K}}(h,\psi)$, and the flux $\overline{\mathcal{G}}^{h} = \overline{\mathcal{G}}(h\overline{u}, \phi + gh)$, $\overline{\mathcal{G}}^{\overline{u}} = \overline{\mathcal{G}}\left(h\overline{u}, \overline{\mathcal{K}}(1,\overline{u})\right)$, $\overline{\mathcal{G}}^{\overline{w}} = \overline{\mathcal{G}}\left(h\overline{u}, \overline{\mathcal{K}}(1,\overline{w})\right)$, and $\overline{\mathcal{G}}^{q_B} = \overline{\mathcal{G}}\left(h\overline{u}, \frac{q_B}{2}\right)$ defined by (3.1).
It is the counterpart of Proposition 1.ii).

3.2.2. Entropy-satisfying numerical scheme of (NH)

Now we focus on the description of a numerical strategy to solve (NH). As in previous works [14, 8, 28, 2, 3], the numerical scheme is based on a splitting between the advection step and the dispersion step. The advantage of this strategy is to use classical scheme (SW^{δ}) for the advection part. The main advantage of the formulation (NH) is to highlight the advection of the vertical velocity (left-hand side). This strategy is was already used in [2, 3] and entropy-satisfying schemes to solve it can be used [9]. However in the cited works, the dispersion step is solved using a prediction correction strategy based on an implicit system on the hydrodynamic pressure q_B. Even if this step dissipate the L^2-norm of the hydrodynamic pressure, the link with the mechanical energy of (NH) is not clear. An other strategy to solve dispersive model is to write the equation on the horizontal velocity see [14, 8, 28]. An advantage of this strategy is that dissipative forces such are friction at the bottom or viscous term can be solve at this step together with the dispersion. For readability, we do not treat this terms in the current work. However, without the introduction of the vertical velocity, this strategy makes appear third order derivatives which are not easy to discretize. The following scheme try to deal with the advantages of the two strategies. More precisely, the vertical velocity is introduce and advected within the hyperbolic step and the dispersion step is solve using the equation on the horizontal velocity. Other strategies based on a new set of variables was proposed in for example [29] but it is not clear how to deal with source term such is bottom variation. To do so, we reformulated (NH) as

$$
\begin{aligned}
&\partial_t \mathcal{U}^{\text{NH}} + \nabla \cdot F^{\text{NH}}\left(\mathcal{U}^{\text{NH}}\right) = S^{\text{NH}}\left(\mathcal{U}^{\text{NH}}\right) + D^{\text{NH}} \\
\text{with} \qquad &\mathcal{U}^{\text{NH}} = \begin{pmatrix} h \\ h\overline{u} \\ h\overline{w} \end{pmatrix}, \qquad F^{\text{NH}}\left(\mathcal{U}^{\text{NH}}\right) = \begin{pmatrix} h\overline{u} \\ h\overline{u} \otimes \overline{u} + \frac{g}{2}h^2 \mathbf{I}_d \\ h\overline{w}\ \overline{u} \end{pmatrix} \\
&S^{\text{NH}}\left(\mathcal{U}^{\text{NH}}\right) = \begin{pmatrix} 0 \\ -h\nabla\phi \\ 0 \end{pmatrix} \quad \text{and} \quad D^{\text{NH}} = \begin{pmatrix} 0 \\ -\nabla\left(h\frac{q_B}{2}\right) - q_B \nabla B \\ q_B \end{pmatrix}.
\end{aligned}
\tag{3.4}
$$

Now assume that the water depth, the horizontal velocity and the vertical velocity at time iteration n are known, i.e. h_k^n, $\overline{u}_k^n$ and $\overline{w}_k^n$, as for exemple at the initial condition. Then the time step can be decomposed into three steps, briefly described as follow:

1. Advection and conservative forces using (SW^{δ}), from now on called the advection step $(NH^{\delta}.\text{a})$.

2. Dispersion and dissipative forces using an implicit finite volume method, from now on called the dispersion step (NH^δ.b).

3. Reconstruction of the vertical velocity $\overline{w}_n^k$, from now on called the reconstruction step (NH^δ.c).

Advection and conservative forces: This step is based on (SW^δ). More precisely, the two first unknowns corresponding to the shallow water unknowns are advected following the strategy (SW^δ) and the vertical velocity $\overline{w}_k^n$ is advected with the mass flux as a passive polutant. This strategy, already used in [2, 3] can be justified as a Suliciu relaxation [39]. We write

$$\mathcal{U}_k^{\text{NH},n+1/2} = \mathcal{U}_k^{\text{NH},n} - \frac{\delta_t^n}{|k|} \sum_{f\in\mathbb{F}_k} \left(\mathcal{F}_f^{\text{NH},n} \cdot \mathcal{N}_k^{\underline{k}_f} + \mathcal{S}_{f,k}^{\text{NH},n} \right) |f| \qquad (NH^\delta\text{.a})$$

with the state vector $\mathcal{U}_k^{\text{NH},n} = (h_k^n,\ h_k^n\overline{u}_k^n,\ h_k^n\overline{w}_k^n)^t$, the numerical flux

$$\mathcal{F}_f^{\text{NH},n} \cdot \mathcal{N}_k^{\underline{k}_f} = \begin{pmatrix} \mathcal{F}_f^{1,n} \cdot \mathcal{N}_k^{\underline{k}_f} \\ \mathcal{F}_f^{2,n} \cdot \mathcal{N}_k^{\underline{k}_f} \\ \overline{w}_k^n \left(\mathcal{F}_f^{1,n} \cdot \mathcal{N}_k^{\underline{k}_f} \right)_+ - \overline{w}_{\underline{k}_f}^n \left(\mathcal{F}_f^{1,n} \cdot \mathcal{N}_k^{\underline{k}_f} \right)_- \end{pmatrix}$$

and source term $\mathcal{S}_{f,k}^{\text{NH},n} = \left(0, \mathcal{S}_{f,k}^{2,n}, 0\right)^t$. The positive and negative part functions are defined by $\phi_\pm = \frac{|\phi|\pm\phi}{2}$.

Dispersion and dissipative forces: Now let us introduce the scheme of the dispersion step. Since the water depth is not affected by this step we set $h_k^{n+1} = h_k^{n+1/2}$. Then anywhere the water depth does not vanishes, the horizontal velocity is corrected solving the following linear implicit scheme

$$\alpha_k^{\text{NH}} \overline{u}_k^{n+1} + \nabla_k^\delta \left(\mu^{\text{NH}} \cdot \overline{u}^{n+1} \right) - \mu_k^{\text{NH}} \nabla_k^\delta \cdot \overline{u}^{n+1} - \nabla_k^\delta \left(\kappa^{\text{NH}} \nabla^\delta \cdot \overline{u}^{n+1} \right) = \beta_k^{\text{NH}} \quad (NH^\delta\text{.b})$$

with the discrete operator ∇_k^δ and $\nabla_k^\delta\cdot$ define by (2.3) and the parameters

$$\alpha_k^{\text{NH}} = h_k^{n+1/2} \left(\mathbf{I}_d + \nabla_k^\delta B^{n+1} \otimes \nabla_k^\delta B^{n+1} \right), \qquad \mu_k^{\text{NH}} = \frac{\left(h_k^{n+1/2}\right)^2}{2} \nabla_k^\delta B^{n+1}, \qquad \kappa_k^{\text{NH}} = \frac{\left(h_k^{n+1/2}\right)^3}{4},$$

and $$\beta_k^{\text{NH}} = h_k^{n+1/2} \overline{u}_k^{n+1/2} + h_k^{n+1/2} \left(\overline{w}_k^{n+1/2} - \partial_t^{n+1} B_k \right) \nabla_k^\delta B^{n+1} + \nabla_k^\delta \left(\frac{\left(h^{n+1/2}\right)^2}{2} \left(\overline{w}^{n+1/2} - \partial_t^{n+1} B \right) \right).$$

Note that in dry area, the scheme leads to a trivial equation. However, the leading linear system is not well-posed. To overcome this drawback, in any dry cell (NH^{δ}.b) is replaced by $\overline{u}_k^{n+1} = 0$. The solution of the dispersion step is obviously affected by the choice of the velocity in the dry areas. However, this choice is motivated by the conservation of the mechanical energy at the dry front, see Proposition 5. More precisely, thanks to this choice flux of energy of the dispersive part vanishes at the dry front. The dissipative forces such are the viscosity or the friction at bottom can easily be considered at this step since they are usually treated using an implicit scheme.

Reconstruction of the vertical velocity: Eventually the vertical velocity is reconstructed. To design an entropy-satisfying scheme, the constrain is discretized by

$$\overline{w}_k^{n+1} = \partial_t^{n+1} B_k + \overline{u}_k^{n+1} \cdot \nabla_k^{\delta} B^{n+1} - \frac{h_k^{n+1}}{2} \nabla_k^{\delta} \cdot \overline{u}^{n+1} \qquad (NH^{\delta}\text{.c})$$

where the discrete time derivative is defined by (2.2) and the discrete operator are defined by (2.3).

Let us give some detail how the scheme is obtained. The reconstruction step scheme is obtained after a rewriting of (NH.b) using the mass conservation (first equation of (NH.a)) as

$$\overline{w} = \partial_t B + \overline{u} \cdot \nabla B - \frac{h}{2} \nabla \cdot \overline{u}$$

to obtain an entropy-satisfying scheme, see Proposition 5. The scheme (NH^{δ}.b) was obtained using an implicit scheme of the dispersion operator in (NH.a) and replacing $\overline{w}_k^{n+1}$ using the reconstruction (NH^{δ}.c). More precisely, the dispersive step of the splitting strategy can be discretized by

$$\mathcal{U}_k^{\mathrm{NH},n+1} = \mathcal{U}_k^{\mathrm{NH},n+1/2} + \delta_t \begin{pmatrix} 0 \\ -\nabla_k^{\delta} \left(h^{n+1} \overline{q}^{n+1} \right) - q_{B,k}^{n+1} \nabla_k^{\delta} B^{n+1} \\ q_{B,k}^{n+1} \end{pmatrix}. \qquad (3.6)$$

Using the reconstruction (NH^{δ}.c) in the third equation of (3.6), the hydrodynamic pressure reads

$$q_{B,k}^{n+1} = \frac{h_k^{n+1/2}}{\delta_t^n} \left(\partial_t^{n+1} B_k + \overline{u}_k^{n+1} \cdot \nabla_k^{\delta} B^{n+1} - \frac{h_k^{n+1/2}}{2} \nabla_k^{\delta} \cdot \overline{u}^{n+1} - \overline{w}_k^{n+1/2} \right) \qquad (3.7)$$

Eventually, we replace $q_{B,k}^{n+1}$ in the second equation of (3.6) to obtain the scheme (NH^δ.b).

Proposition 5. *Let (SW^δ) satisfies Proposition 3.*
Assuming $h_k^0 \geq 0$ and the CFL condition (3.2) holds. Then the solution of (NH^δ) satisfies

5.i) the positivity of the water depth, i.e. $h_k^n \geq 0$.
It is the discrete counterpart of Proposition 4.i).

5.ii) the following mechanical energy dissipation

$$\partial_t^{n+1}\left(\mathcal{E}_k + \overline{\mathcal{K}}_k^{\overline{u}} + \overline{\mathcal{K}}_k^{\overline{w}}\right) + \tfrac{1}{|k|}\textstyle\sum_{f\in\mathbb{F}_k}\left(\overline{\mathcal{G}}_f^{h,n} + \overline{\mathcal{G}}_f^{\overline{u},n} + \overline{\mathcal{G}}_f^{\overline{w},n} + \overline{\mathcal{G}}_f^{q_B,n+1}\right)\cdot\mathcal{N}_k^{\underline{k}_f}\,|f| \leq h_k^n\partial_t^{n+1}\phi_k + q_{B,k}^{n+1}\partial_t^{n+1}B_k$$

with the energies $\mathcal{E}_k^n = \mathcal{E}\left(h_k^n\right)$, $\overline{\mathcal{K}}_k^{\psi,n} = \overline{\mathcal{K}}\left(h_k^n,\psi_k^n\right)$ defined by (3.1) and the flux $\overline{\mathcal{G}}_f^{h,n} = \overline{\mathcal{G}}_\delta^h\left(\mathcal{U}_k^{\mathrm{NH},n},\mathcal{U}_{\underline{k}_f}^{\mathrm{NH},n}\right)$, $\overline{\mathcal{G}}_f^{\overline{u},n} = \overline{\mathcal{G}}_\delta^{\overline{u}}\left(\mathcal{U}_k^{\mathrm{NH},n},\mathcal{U}_{\underline{k}_f}^{\mathrm{NH},n}\right)$ introduced in Proposition 3.ii), $\overline{\mathcal{G}}_f^{\overline{w},n} = \overline{\mathcal{G}}_\delta^{up}\left(\mathcal{F}_f^{1,n}\cdot\mathcal{N}_k^{\underline{k}_f},\overline{w}_k^n,\overline{w}_{\underline{k}_f}^n\right)$ with

$$\overline{\mathcal{G}}_\delta^{up}\left(\mathcal{F},\psi_L,\psi_R\right) = \frac{g}{2}\left(\psi_L^2\mathcal{F}_+ - \psi_R^2\mathcal{F}_-\right)$$

and $\overline{\mathcal{G}}_f^{q_B,n} = \overline{\mathcal{G}}_\delta^{\overline{q}}\left(h_k^n,\overline{u}_k^n,\dfrac{q_{B,k}^n}{2};h_{\underline{k}_f}^n,\overline{u}_{\underline{k}_f}^n,\dfrac{q_{B,\underline{k}_f}^n}{2}\right)$ defined by

$$\overline{\mathcal{G}}_\delta^{\overline{q}}\left(h_L,u_L,\overline{q}_L;h_R,u_R,\overline{q}_R\right) = \frac{h_L\overline{q}_L + h_R\overline{q}_R}{2}\frac{\overline{u}_L+\overline{u}_R}{2} - \frac{h_R\overline{q}_R - h_L\overline{q}_L}{2}\frac{\overline{u}_R-\overline{u}_L}{2}.$$

It is the discrete counterpart of Proposition 4.ii).

Proof. Proposition 5.i) is an obvious consequence of Proposition 3.i).
Let us focus on the mechanical energy conservation Proposition 7.ii). The advection step (NH^δ.a) is a shallow water scheme (SW^δ) for the first unknowns h and $h\overline{u}$. Thanks to Proposition 3.ii), we have

$$\mathcal{E}_k^{n+1/2} + \overline{\mathcal{K}}_k^{\overline{u},n+1/2} + \frac{\delta_t^n}{|k|}\sum_{f\in\mathbb{F}_k}\left(\overline{\mathcal{G}}_f^{h,n} + \overline{\mathcal{G}}_f^{\overline{u},n}\right)\cdot\mathcal{N}_k^{\underline{k}_f}\,|f| \leq \mathcal{E}_k^n + \overline{\mathcal{K}}_k^{\overline{u},n} + h_k^n\left(\phi_k^{n+1} - \phi_k^n\right) \tag{3.8}$$

with $\mathcal{E}_k^{n+1/2} = \mathcal{E}\left(h_k^{n+1/2}\right)$ and $\overline{\mathcal{K}}_k^{\psi,n+1/2} = \overline{\mathcal{K}}\left(h_k^{n+1/2}, \psi_k^{n+1/2}\right)$.
Since the advection of $\overline{w}_k^n$ is a classical up-wind scheme with the mass flux and the positivity is already ensured Proposition 5.i), we conclude the following entropy inequality, see [9, Chapter 2.7]

$$\overline{\mathcal{K}}_k^{\overline{w},n+1/2} + \frac{\delta_t}{|k|} \sum_{f \in \mathbb{F}_k} \overline{\mathcal{G}}_f^{\overline{w},n} |f| \leq \overline{\mathcal{K}}_k^{\overline{w},n}. \tag{3.9}$$

Now we focus on the dispersion step (NH^δ.b) and proceed similarly to the continuous case. More precisely as it was previously explained, the dispersion step can be written as (3.6), (3.7) and (NH^δ.c). Now multiplying the second equation of (3.6) by $\overline{u}_k^{n+1}$, it reads

$$\overline{\mathcal{K}}_k^{\overline{u},n+1} \leq \overline{\mathcal{K}}_k^{\overline{u},n+1/2} - \delta_t^n \left(\overline{u}_k^{n+1} \cdot \nabla_k^\delta \left(h^{n+1} \frac{q_B^{n+1}}{2} \right) + q_{B,k}^{n+1} \overline{u}_k^{n+1} \cdot \nabla_k^\delta B^{n+1} \right). \tag{3.10}$$

Thanks to the centered operator (2.3), we have

$$\overline{u}_k^{n+1} \cdot \nabla_k^\delta \left(h^{n+1} \frac{q_B^{n+1}}{2} \right) = \frac{1}{|k|} \sum_{f \in \mathbb{F}_k} \overline{\mathcal{G}}_f^{q_B,n+1} \cdot \mathcal{N}_k^{\underline{k}_f} |f| - q_{B,k}^{n+1} \frac{h_k^{n+1}}{2} \nabla_k^\delta \cdot \overline{u}^{n+1}.$$

Then multiplying the third equation of (3.6) by $\overline{w}_k^{n+1}$, it reads

$$\overline{\mathcal{K}}_k^{\overline{w},n+1} \leq \overline{\mathcal{K}}_k^{\overline{w},n+1/2} + \delta_t^n q_{B,k}^{n+1} \overline{w}_k^{n+1}. \tag{3.11}$$

Summing the energy dissipations (3.10) and (3.11), it yields

$$\begin{aligned} \overline{\mathcal{K}}_k^{\overline{u},n+1} + \overline{\mathcal{K}}_k^{\overline{w},n+1} + \frac{\delta_t^n}{|k|} \sum_{f \in \mathbb{F}_k} \overline{\mathcal{G}}_f^{q_B,n+1} \cdot \mathcal{N}_k^{\underline{k}_f} |f| \leq \overline{\mathcal{K}}_k^{\overline{u},n+1/2} + \overline{\mathcal{K}}_k^{\overline{w},n+1/2} \\ + \delta_t^n q_{B,k}^{n+1} \left(\overline{w}_k^{n+1} - \overline{u}_k^{n+1} \cdot \nabla_k^\delta B^{n+1} + \frac{h_k^{n+1}}{2} \nabla_k^\delta \cdot \overline{u}^{n+1} \right). \end{aligned} \tag{3.12}$$

The last term can be written as the discrete time derivative of the bottom using (NH^δ.c). Since $h_k^{n+1/2} = h_k^{n+1}$ we have $\mathcal{E}_k^{n+1/2} = \mathcal{E}_k^{n+1}$ and we conclude summing (3.8) with (3.12). Note that at the wet/dry front, the flux of energy $\overline{\mathcal{G}}_\delta^{\overline{q},n+1}$ vanishes setting the horizontal velocity to zero in the dry cell. More precisely, since the water level vanish in one cell, for instead $h_R = 0$, the flux is proportional to the the velocity in the velocity in the dry cell $\overline{u}_R$. □

Remark 5.1. *A drawback of* (NH^δ) *is the large stencil of the dispersion operator* (NH^δ.b)*, i.e. 5-point stencil in 1D. Some can replace* (NH^δ.b) *by a more compact and simpler discrete operator, see Appendix Appendix B. However, the entropy dissipation Proposition 5.ii) is lost and in practice the numerical results are less accurate, see §5.3.*

3.3. Serre-Green-Naghdi model (*GN*)

3.3.1. Governing equations of (*GN*) *and main properties*

We now deal with the Serre-Green-Naghdi model [38, 34, 22]. To proposed a scheme in the spirit of (NH^δ), the Serre-Green-Naghdi model is reformulated as follow

$$\begin{cases} \partial_t h & + \nabla \cdot (h\overline{u}) & = 0 \\ \partial_t (h\overline{u}) & + \nabla \cdot \left(h\overline{u} \otimes \overline{u} + \dfrac{g}{2} h^2 \mathbf{I}_d \right) & = -h\nabla\phi - \nabla (h\overline{q}) - q_B \nabla B \\ \partial_t (h\overline{w}) & + \nabla \cdot (h\overline{w}\ \overline{u}) & = q_B \\ \partial_t (h\sigma) & + \nabla \cdot (h\sigma\ \overline{u}) & = \sqrt{3}\,(2\overline{q} - q_B) \end{cases} \tag{GN.a}$$

with two constrains associated to the Lagrange multipliers $\overline{q}$ and q_B reads

$$\overline{w} = \partial_t \left(B + \frac{h}{2} \right) + \overline{u} \cdot \nabla \left(B + \frac{h}{2} \right) \quad \text{and} \quad \sigma = \frac{\partial_t h + \overline{u} \cdot \nabla h}{2\sqrt{3}}. \tag{GN.b}$$

An initial condition is required on $h\,(0,x) = h^0\,(x)$, $\overline{u}\,(0,x) = \overline{u}^0\,(x)$, $\overline{w}\,(0,x) = \overline{w}^0\,(x)$ and $\sigma\,(0,x) = \sigma^0\,(x)$ and have to satisfy the compatibility conditions

$$\overline{w}^0 = \partial_t B_{|_{t=0}} + \overline{u}^0 \cdot \nabla B - \frac{h^0}{2} \nabla \cdot \overline{u}^0 \qquad \text{and} \qquad \sigma^0 = -\frac{h^0}{2\sqrt{3}} \nabla \cdot \overline{u}^0$$

which in no more than a rewriting of the constrains (*GN*.b) at the initial time using the conservation of mass. In [18] it is shown that (*GN*) is equivalent, at least for smooth solution, to the classical Peregrine formulation [34]. A formal derivation of (*GN*) is presented in §Appendix A. Let us first recall the main physical properties of (*GN*).

Proposition 6. *Assuming that* $h^0\,(x) \geq 0$*,*
then the solution of (*GN*) *satisfies*

6.i) the positivity of the water depth, i.e. $h\,(t,x) \geq 0$.
It is the counterpart of Proposition 1.i).

6.ii) the following mechanical energy balance for smooth enough solution

$$\partial_t\left(\mathcal{E}+\overline{\mathcal{K}}^{\overline{u}}+\overline{\mathcal{K}}^{\overline{w}}+\overline{\mathcal{K}}^{\sigma}\right)+\nabla\cdot\left(\overline{\mathcal{G}}^{h}+\overline{\mathcal{G}}^{\overline{u}}+\overline{\mathcal{G}}^{\overline{w}}+\overline{\mathcal{G}}^{\sigma}+\overline{\mathcal{G}}^{\overline{q}}\right)=h\partial_t\phi+q_B\partial_t B$$

with the potential energy $\mathcal{E}(h)$ *defined by* (2.1)*, the kinetic energies* $K^{\psi}=\overline{\mathcal{K}}(h,\psi)$ *and the flux* $\overline{\mathcal{G}}^{h}=\overline{\mathcal{G}}(h\overline{u},\phi+gh)$*,* $\overline{\mathcal{G}}^{\overline{u}}=\overline{\mathcal{G}}\left(h\overline{u},\overline{\mathcal{K}}(1,\overline{u})\right)$*,* $\overline{\mathcal{G}}^{\overline{w}}=\overline{\mathcal{G}}\left(h\overline{u},\overline{\mathcal{K}}(1,\overline{w})\right)$*,* $\overline{\mathcal{G}}^{\sigma}=\overline{\mathcal{G}}\left(h\overline{u},\overline{\mathcal{K}}(1,\sigma)\right)$*,* $\overline{\mathcal{G}}^{\overline{q}}=\overline{\mathcal{G}}(h\overline{u},\overline{q})$ *defined by* (3.1)*.*
It is the counterpart of Proposition 1.ii).

3.3.2. Entropy-satisfying numerical scheme of (*GN*)

Now we focus on the description of a numerical strategy to solve (*GN*). Similarly to (NH^{δ}), (*GN*.a) is written as

$$\partial_t\mathcal{U}^{\mathrm{GN}}+\nabla\cdot F^{\mathrm{GN}}(\mathcal{U}^{\mathrm{GN}})=S^{\mathrm{GN}}(\mathcal{U}^{\mathrm{GN}})+D^{\mathrm{GN}}$$

$$\text{with}\qquad \mathcal{U}^{\mathrm{GN}}=\begin{pmatrix}h\\ h\overline{u}\\ h\overline{w}\\ h\sigma\end{pmatrix},\qquad F^{\mathrm{GN}}(\mathcal{U}^{\mathrm{GN}})=\begin{pmatrix}h\overline{u}\\ h\overline{u}\otimes\overline{u}+\frac{g}{2}h^2\mathbf{I}_d\\ h\overline{w}\ \overline{u}\\ h\sigma\ u\end{pmatrix}$$

$$S^{\mathrm{GN}}(\mathcal{U}^{\mathrm{GN}})=\begin{pmatrix}0\\ -h\nabla\phi\\ 0\\ 0\end{pmatrix}\quad\text{and}\quad D^{\mathrm{GN}}=\begin{pmatrix}0\\ -\nabla(h\overline{q})-q_B\nabla B\\ q_B\\ \sqrt{3}(2\overline{q}-q_B)\end{pmatrix}$$

and the numerical strategy is based on the same three step : advection and conservative forces, dispersion and dissipative forces, reconstruction of the vertical velocity.

Advection and conservative forces: As done for (NH^{δ}.a), the advection and conservative forces are realized using the strategy (SW^{δ}) with an up-wind scheme for the vertical velocities $\overline{w}_k^n$ and σ_k^n. We write

$$\mathcal{U}_k^{\mathrm{GN},n+1/2}=\mathcal{U}_k^{\mathrm{GN},n}-\frac{\delta_t^n}{|k|}\sum_{f\in\mathbb{F}_k}\left(\mathcal{F}_f^{\mathrm{GN},n}\cdot\mathcal{N}_k^{k_f}+\mathcal{S}_{f,k}^{\mathrm{GN},n}\right)|f| \qquad (GN^{\delta}.\mathrm{a})$$

with the state vectors $\mathcal{U}_k^{\mathrm{GN},n} = (h_k^n,\ h_k^n\overline{u}_k^n,\ h_k^n\overline{w}_k^n,\ h_k^n\sigma_k^n)^t$, the numerical flux and source term

$$\mathcal{F}_f^{\mathrm{GN},n}\cdot\mathcal{N}_k^{\underline{k}_f} = \begin{pmatrix} \mathcal{F}_f^{1,n}\cdot\mathcal{N}_k^{\underline{k}_f} \\ \mathcal{F}_f^{2,n}\cdot\mathcal{N}_k^{\underline{k}_f} \\ \overline{w}_k^n\left(\mathcal{F}_f^{1,n}\cdot\mathcal{N}_k^{\underline{k}_f}\right)_+ - \overline{w}_{\underline{k}_f}^n\left(\mathcal{F}_f^{1,n}\cdot\mathcal{N}_k^{\underline{k}_f}\right)_- \\ \sigma_k^n\left(\mathcal{F}_f^{1,n}\cdot\mathcal{N}_k^{\underline{k}_f}\right)_+ - \sigma_{\underline{k}_f}^n\left(\mathcal{F}_f^{1,n}\cdot\mathcal{N}_k^{\underline{k}_f}\right)_- \end{pmatrix}$$

and the source term $\mathcal{S}_{f,k}^{\mathrm{GN},n} = \left(0, \mathcal{S}_{f,k}^{2,n}, 0, 0\right)^t$.

Dispersion and dissipative forces: Now let us introduce the scheme of the dispersion step. We set $h_k^{n+1} = h_k^{n+1/2}$ and in any wet cell

$$\alpha_k^{\mathrm{GN}}\overline{u}_k^{n+1} + \nabla_k^\delta\left(\mu^{\mathrm{GN}}\cdot\overline{u}^{n+1}\right) - \mu_k^{\mathrm{GN}}\nabla_k^\delta\cdot\overline{u}^{n+1} - \nabla_k^\delta\left(\kappa^{\mathrm{GN}}\nabla^\delta\cdot\overline{u}^{n+1}\right) = \beta_k^{\mathrm{GN}} \quad (GN^\delta.\mathrm{b})$$

where the parameters read

$$\alpha_k^{\mathrm{GN}} = h_k^{n+1/2}\left(\mathbf{I}_d + \nabla_k^\delta B^{n+1}\otimes\nabla_k^\delta B^{n+1}\right), \quad \mu_k^{\mathrm{GN}} = \frac{\left(h_k^{n+1/2}\right)^2}{2}\nabla_k^\delta B^{n+1}, \quad \kappa_k^{\mathrm{GN}} = \frac{\left(h_k^{n+1/2}\right)^3}{3} \quad \text{and}$$

$$\beta_k^{\mathrm{GN}} = h_k^{n+1/2}\overline{u}_k^{n+1/2} + h_k^{n+1/2}\left(\overline{w}_k^{n+1/2} - \partial_t^{n+1}B_k\right)\nabla_k^\delta B^{n+1} + \nabla_k^\delta\left(\frac{\left(h^{n+1/2}\right)^2}{2}\left(\overline{w}^{n+1/2} + \frac{\sigma^{n+1/2}}{\sqrt{3}} - \partial_t^{n+1}B\right)\right)$$

Similarly to (NH^δ), in dry cell we set $\overline{u}_k^{n+1} = 0$ and the dissipative forces can also be considered at this step.

Reconstruction of the vertical velocity: In this step we reconstruct the vertical velocity. As done for $(NH^\delta.\mathrm{c})$, we set

$$\overline{w}_k^{n+1} = \partial_t^{n+1}B_k + \overline{u}_k^{n+1}\cdot\nabla_k^\delta B^{n+1} - \frac{h_k^{n+1}}{2}\nabla_k^\delta\cdot\overline{u}^{n+1} \qquad \text{and} \qquad \sigma_k^{n+1} = -\frac{h_k^{n+1}}{2\sqrt{3}}\nabla_k^\delta\cdot\overline{u}^{n+1}. \quad (GN^\delta.\mathrm{c})$$

The scheme $(GN^\delta.\mathrm{b})$ was obtained similarly to $(NH^\delta.\mathrm{b})$. More precisely, the reconstruction step scheme is obtained after a rewriting of $(GN.\mathrm{b})$ using the mass conservation (first equation of $(GN.\mathrm{a})$) as

$$\overline{w} = \partial_t B + \overline{u}\cdot\nabla B - \frac{h}{2}\nabla\cdot\overline{u} \qquad \text{and} \qquad \sigma = -\frac{h}{2\sqrt{3}}\nabla\cdot\overline{u}$$

to obtain an entropy-satisfying scheme, see Proposition 7. Then, we set

$$\mathcal{U}_k^{\mathrm{GN},n+1} = \mathcal{U}_k^{\mathrm{GN},n+1/2} + \delta_t \begin{pmatrix} 0 \\ -\nabla_k^\delta \left(h^{n+1} \overline{q}^{n+1} \right) - q_{B,k}^{n+1} \nabla_k^\delta B^{n+1} \\ q_{B,k}^{n+1} \\ \sqrt{3} \left(2\overline{q}_k^{n+1} - q_{B,k}^{n+1} \right) \end{pmatrix} \tag{3.15}$$

Using the reconstruction (GN^δ.c) in the third and fourth equations of (3.15), the hydrodynamic pressure reads

$$q_{B,k}^{n+1} = \frac{h_k^{n+1/2}}{\delta_t^n} \left(\partial_t^{n+1} B_k + \overline{u}_k^{n+1} \cdot \nabla_k^\delta B^{n+1} - \frac{h_k^{n+1/2}}{2} \nabla_k^\delta \cdot \overline{u}^{n+1} - \overline{w}_k^{n+1/2} \right)$$

and

$$\overline{q}_k^{n+1} = \frac{h_k^{n+1/2}}{2\delta_t^n} \left(\partial_t^{n+1} B_k + \overline{u}_k^{n+1} \cdot \nabla_k^\delta B^{n+1} - \frac{2h_k^{n+1/2}}{3} \nabla_k^\delta \cdot \overline{u}^{n+1} - \left(\overline{w}_k^{n+1/2} + \frac{\sigma_k^{n+1/2}}{\sqrt{3}} \right) \right).$$

Eventually, we replace $\overline{q}_k^{n+1}$ and $q_{B,k}^{n+1}$ in the second equation of (3.15) to obtain the scheme (GN^δ.b).

Proposition 7. *Let (SW^δ) satisfies Proposition 3.*
Assuming $h_k^0 \geq 0$ and the CFL condition (3.2) holds. Then the solution of (GN^δ) satisfies

7.i) the positivity of the water depth, i.e. $h_k^n \geq 0$.
It is the discrete counterpart of Proposition 6.i).

7.ii) the following mechanical energy dissipation

$$\partial_t^{n+1} \left(\mathcal{E}_k + \overline{\mathcal{K}}_k^{\overline{u}} + \overline{\mathcal{K}}_k^{\overline{w}} + \overline{\mathcal{K}}_k^{\sigma} \right) + \frac{1}{|k|} \sum_{f \in \mathbb{F}_k} \left(\overline{\mathcal{G}}_f^{h,n} + \overline{\mathcal{G}}_f^{\overline{u},n} + \overline{\mathcal{G}}_f^{\overline{w},n} + \overline{\mathcal{G}}_f^{\sigma,n} + \overline{\mathcal{G}}_f^{\overline{q},n+1} \right) \cdot \mathcal{N}_k^{\underline{k}_f} |f| \leq h_k^n \partial_t^{n+1} \phi_k + q_{B,k}^{n+1} \partial_t^{n+1} B_k$$

with the energies $\mathcal{E}_k^n = \mathcal{E}(h_k^n)$, $\overline{\mathcal{K}}_k^{\psi,n} = \overline{\mathcal{K}}(h_k^n, \psi_k^n)$ defined by (3.1), the flux $\overline{\mathcal{G}}_f^{h,n} = \overline{\mathcal{G}}_\delta^h \left(\mathcal{U}_k^{\mathrm{NH},n}, \mathcal{U}_{\underline{k}_f}^{\mathrm{NH},n} \right)$, $\overline{\mathcal{G}}_f^{\overline{u},n} = \overline{\mathcal{G}}_\delta^{\overline{u}} \left(\mathcal{U}_k^{\mathrm{NH},n}, \mathcal{U}_{\underline{k}_f}^{\mathrm{NH},n} \right)$ introduced in Proposition 3.ii), $\overline{\mathcal{G}}_f^{\overline{w},n} = \overline{\mathcal{G}}_\delta^{up} \left(\mathcal{F}_f^{1,n} \cdot \mathcal{N}_k^{\underline{k}_f}, \overline{w}_k^n, \overline{w}_{\underline{k}_f}^n \right)$, $\overline{\mathcal{G}}_f^{\sigma,n} = \overline{\mathcal{G}}_\delta^{up} \left(\mathcal{F}_f^{1,n} \cdot \mathcal{N}_k^{\underline{k}_f}, \sigma_k^n, \sigma_{\underline{k}_f}^n \right)$ and $\overline{\mathcal{G}}_f^{\overline{q},n} = \overline{\mathcal{G}}_\delta^{\overline{q}} \left(h_k^n, \overline{u}_k^n, \overline{q}_{B,k}^n; h_{\underline{k}_f}^n, \overline{u}_{\underline{k}_f}^n, \overline{q}_{B,\underline{k}_f}^n \right)$ where the functions $\overline{\mathcal{G}}_\delta^{up}$ and $\overline{\mathcal{G}}_f^{\overline{q}}$ are introduced in Proposition 5.ii).
It is the discrete counterpart of Proposition 6.ii).

Proof. Proposition 7.i) is an obvious consequence of Proposition 3.i).
Let us focus on the mechanical energy conservation Proposition 7.ii). The proof is similar to the one of Proposition 5.ii). Thanks to Proposition 3.ii), we obtain (3.8). Using the properties of the up-wind scheme, we obtain (3.9) and

$$\overline{\mathcal{K}}_k^{\sigma,n+1/2} + \frac{\delta_t}{|k|} \sum_{f\in\mathbb{F}_k} \overline{\mathcal{G}}_f^{\sigma,n} |f| \leq \overline{\mathcal{K}}_k^{\sigma,n}.$$

Now multiplying the second equation of (3.15) by $\overline{u}_k^{n+1}$, instead of (3.10) it reads

$$\overline{\mathcal{K}}_k^{\overline{u},n+1} + \frac{\delta_t^n}{|k|} \sum_{f\in\mathbb{F}_k} \overline{\mathcal{G}}_f^{\overline{q},n+1} \cdot \mathcal{N}_k^{\underline{k}_f} |f| \leq \overline{\mathcal{K}}_k^{\overline{u},n+1/2} - \delta_t^n \left(-\overline{q}_k^{n+1} h_k^{n+1} \nabla_k^\delta \cdot \overline{u}^{n+1} + q_{B,k}^{n+1} \overline{u}_k^{n+1} \cdot \nabla_k^\delta B^{n+1} \right). \tag{3.16}$$

Then multiplying the third equation of (3.15) by $\overline{w}_k^{n+1}$, we get (3.11) and the fourth by σ_k^{n+1}, we get

$$\overline{\mathcal{K}}_k^{\sigma,n+1} \leq \overline{\mathcal{K}}_k^{\sigma,n+1/2} + \delta_t^n \sqrt{3} \left(2\overline{q}_k^{n+1} - q_{B,k}^{n+1} \right) \sigma_k^{n+1} \tag{3.17}$$

Summing the energy dissipations (3.16), (3.11) and (3.17), it yields

$$\begin{aligned} \overline{\mathcal{K}}_k^{\overline{u},n+1} + \overline{\mathcal{K}}_k^{\overline{w},n+1} + \overline{\mathcal{K}}_k^{\sigma,n+1} + \frac{1}{|k|} \sum_{f\in\mathbb{F}_k} \overline{\mathcal{G}}_f^{\overline{q},n+1} \cdot \mathcal{N}_k^{\underline{k}_f} |f| \leq \overline{\mathcal{K}}_k^{\overline{u},n+1/2} + \overline{\mathcal{K}}_k^{\overline{w},n+1/2} + \overline{\mathcal{K}}_k^{\sigma,n+1/2} \\ + \delta_t 2\sqrt{3} \overline{q}_k^{n+1} \left(\sigma_k^{n+1} + \frac{h_k^{n+1}}{2\sqrt{3}} \nabla_k^\delta \cdot \overline{u}^{n+1} \right) + \delta_t^n q_{B,k}^{n+1} \left(\overline{w}_k^{n+1} - \left(\overline{u}_k^{n+1} \cdot \nabla_k^\delta B^{n+1} + \sqrt{3} \sigma_k^{n+1} \right) \right). \end{aligned}$$

We conclude using (GN^δ.c) and summing with (3.8). □

As it was remark for the scheme (NH^δ), (GN^δ) can be replaced by a more compact and simpler discrete operator, see Appendix Appendix B. However, the discrete dissipation of the mechanical energy is lost and the scheme is less accurate, see §5.3.

4. Some boundary conditions

In the current section, a simple treatment of the boundary conditions is presented. The boundary condition are presented for (GN^δ) because it is the more complexe model but can be easily adapted for (NH^δ). It is not clear even at the continuous level what boundary conditions are consistant

with the model (GN). The current section is only devoted to the numerical treatment of the boundary condition, i.e. which conditions are required by the numerical scheme and how they are prescribed. It is not clear that the strategy details here is completely consistant with the continuous framework and a devoted analysis is required. A fine analysis for transparent boundary condition for (GN) is realized in [25].

In the first hand, explicit schemes generally use the ghost cell strategy, i.e. it impose a value of the state variable immediately after the bound. In the other hand, implicit scheme generally use condition which have to be taking into account inside the linear system and depend on the solution. Now it is not clear how to impose the boundary condition such that both steps (advection and dispersion) are consistant. In particular, the boundary condition of the advection step is define neglecting the dispersive effect, i.e. using Riemann invariant. This strategy seems limited to the case where the dispersive effect are small at the bound.

The set $\partial\mathbb{F}$ is the set of face at the boundary and $\widetilde{f} \in \partial\mathbb{F}$ is on the border whereas the cell $\widetilde{k}$ is in the computational domain and its neighbor $\underline{\widetilde{k}}_{\widetilde{f}}$ is the ghost cell.

4.1. Boundary conditions for the advection step

The advection step consists of the resolution of a system of hyperbolic equations. The number of information that have to be impose depends on the regime of the flow, subcritical, i.e. $Fr < 1$ or supercritical, i.e. $Fr > 1$ with the Froude number normal to the bound defined by $Fr = \frac{\left\| \overline{u}^n_{\widetilde{k}} \cdot \mathcal{N}^{\widetilde{k}\widetilde{f}}_{\widetilde{k}} \right\|}{\sqrt{g h^n_{\widetilde{k}}}}$. In the subcritical case, two type of condition are usually considered, either the water depth is imposed, either the discharge is imposed. The so-called wall boundary, where mass flux vanishes at the bound, is largely use in practice. In the supercritical case, the whole state variables have to be given if the flow is incoming but else no information can to be imposed. This list is not exhaustive and several other type of boundary conditions can be considered, see [20, Chapter V]. In addition to the boundary conditions imposed to the classical shallow water model, the vertical velocity ($\overline{w}^n_{\underline{\widetilde{k}}_{\widetilde{f}}}$ in the case of (NH^δ) or $\overline{w}^n_{\underline{\widetilde{k}}_{\widetilde{f}}}$ and $\sigma^n_{\underline{\widetilde{k}}_{\widetilde{f}}}$ in the case of (GN^δ)) have to be prescribed iff the mass flux is incoming, i.e. $\mathcal{F}^{1,n}_{\widetilde{f}} \cdot \mathcal{N}^{\widetilde{k}\widetilde{f}}_{\widetilde{k}} < 0$.

4.2. Boundary conditions for the dispersion step

Thanks to the ghost cell, the advection step (GN^{δ}.a) as well as the reconstruction step (GN^{δ}.c) are computable in the whole computational domain. Let us now focus on the dispersive step (GN^{δ}.b). Even if the horizontal velocity $\overline{u}^{n+1}_{\underline{\widetilde{k}}_{\widetilde{f}}}$ is already known, the scheme also required the vertical velocity $\overline{w}^{n+1/2}_{\underline{\widetilde{k}}_{\widetilde{f}}}$ and $\sigma^{n+1/2}_{\underline{\widetilde{k}}_{\widetilde{f}}}$. Moreover, due to the large stencil of the scheme, the horizontal velocity is also required in the neighbor of $\underline{\widetilde{k}}_{\widetilde{f}}$ and need some geometrical informations such are the surface area of $\underline{\widetilde{k}}_{\widetilde{f}}$. It is clearly not suitable that the numerical simulation depends on this quantities. To overcome this drawback, we back to the formulation (3.15) where it is clear that only $\overline{q}^{n+1}_{\underline{\widetilde{k}}_{\widetilde{f}}}$ is actually required. The strategy to impose the hydrodynamic pressure at the boundary was already propose in [2, 3]. It is not clear how the hydrodynamic pressure at the boundary should be link to the other knowns already defined. In the current paper, we only details the Neumann condition $\overline{q}^{n+1}_{\underline{\widetilde{k}}_{\widetilde{f}}} = \overline{q}^{n+1}_{\widetilde{k}}$. Other boundary conditions was tested: Dirichlet condition $\overline{q}^{n+1}_{\underline{\widetilde{k}}_{\widetilde{f}}} = 0$ or Neumann condition $h^{n+1}_{\underline{\widetilde{k}}_{\widetilde{f}}}\overline{q}^{n+1}_{\underline{\widetilde{k}}_{\widetilde{f}}} = h^{n+1}_{\widetilde{k}}\overline{q}^{n+1}_{\widetilde{k}}$, and leads to similar results in practice. More precisely, starting from (3.15) with $\overline{q}^{n+1}_{\underline{\widetilde{k}}_{\widetilde{f}}} = \overline{q}^{n+1}_{\widetilde{k}}$, the scheme in the last cell $\widetilde{k}$ reads

$$\alpha^{\mathrm{GN}}_{\widetilde{k}}\overline{u}^{n+1}_{\widetilde{k}} + \frac{1}{2\left|\widetilde{k}\right|}\left(\sum_{f\in\mathbb{F}_{\widetilde{k}}\setminus\partial\mathbb{F}} \mu^{\mathrm{GN}}_{\underline{\widetilde{k}}_f}\cdot\overline{u}^{n+1}_{\underline{\widetilde{k}}_f}\mathcal{N}^{\underline{\widetilde{k}}_f}_{\widetilde{k}}|f| + \sum_{\widetilde{f}\in\mathbb{F}_{\widetilde{k}}\cap\partial\mathbb{F}} \mu^{\mathrm{GN}}_{\underline{\widetilde{k}}_{\widetilde{f}}}\cdot\overline{u}^{n+1}_{\widetilde{k}}\mathcal{N}^{\underline{\widetilde{k}}_{\widetilde{f}}}_{\widetilde{k}}\left|\widetilde{f}\right|\right)$$
$$-\mu^{\mathrm{GN}}_{\widetilde{k}}\nabla^{\delta}_{\widetilde{k}}\cdot\overline{u}^{n+1} - \frac{1}{2\left|\widetilde{k}\right|}\left(\sum_{f\in\mathbb{F}_{\widetilde{k}}\setminus\partial\mathbb{F}} \kappa^{\mathrm{GN}}_{\underline{\widetilde{k}}_f}\nabla^{\delta}_{\underline{\widetilde{k}}_f}\cdot\overline{u}^{n+1}\mathcal{N}^{\underline{\widetilde{k}}_f}_{\widetilde{k}}|f| + \sum_{\widetilde{f}\in\mathbb{F}_{\widetilde{k}}\cap\partial\mathbb{F}} \kappa^{\mathrm{GN}}_{\underline{\widetilde{k}}_{\widetilde{f}}}\nabla^{\delta}_{\widetilde{k}}\cdot\overline{u}^{n+1}\mathcal{N}^{\underline{\widetilde{k}}_{\widetilde{f}}}_{\widetilde{k}}\left|\widetilde{f}\right|\right) = \widetilde{\beta}^{\mathrm{GN}}_{\widetilde{k}}$$

with the parameters $\alpha_{\widetilde{k}}^{\mathrm{GN}}$, $\mu_{\widetilde{k}}^{\mathrm{GN}}$ and $\kappa_{\widetilde{k}}^{\mathrm{GN}}$ defined in (GN^{δ}.b),

$$\underline{\mu_{\widetilde{k}}^{\mathrm{GN}}}_{\widetilde{f}} = \frac{h_{\underline{\widetilde{k}}_{\widetilde{f}}}^{n+1} h_{\widetilde{k}}^{n+1/2}}{2} \nabla_{\widetilde{k}}^{\delta} B^{n+1}, \qquad \underline{\kappa_{\widetilde{k}}^{\mathrm{GN}}}_{\widetilde{f}} = \frac{h_{\underline{\widetilde{k}}_{\widetilde{f}}}^{n+1} \left(h_{\widetilde{k}}^{n+1/2}\right)^2}{3} \qquad \text{and}$$

$$\begin{aligned}
\widetilde{\beta}_{\widetilde{k}}^{\mathrm{GN}} &= h_{\widetilde{k}}^{n+1/2} \overline{u}_{\widetilde{k}}^{n+1/2} + h_{\widetilde{k}}^{n+1/2} \left(\overline{w}_{\widetilde{k}}^{n+1/2} - \partial_t^{n+1} B_{\widetilde{k}}\right) \nabla_{\widetilde{k}}^{\delta} B^{n+1} \\
&\quad + \frac{1}{4\left|\widetilde{k}\right|} \left(\sum_{f \in \mathbb{F}_{\widetilde{k}} \setminus \partial\mathbb{F}} \left(h_{\underline{\widetilde{k}}_f}^{n+1/2}\right)^2 \left(\overline{w}_{\underline{\widetilde{k}}_f}^{n+1/2} + \frac{\sigma_{\underline{\widetilde{k}}_f}^{n+1/2}}{\sqrt{3}} - \partial_t^{n+1} B_{\underline{\widetilde{k}}_f} \right) \mathcal{N}_{\widetilde{k}}^{\underline{\widetilde{k}}_f} |f| \right. \\
&\quad \left. + \sum_{\widetilde{f} \in \mathbb{F}_{\widetilde{k}} \cap \partial\mathbb{F}} h_{\underline{\widetilde{k}}_{\widetilde{f}}}^{n+1} h_{\widetilde{k}}^{n+1/2} \left(\overline{w}_{\widetilde{k}}^{n+1/2} + \frac{\sigma_{\widetilde{k}}^{n+1/2}}{\sqrt{3}} - \partial_t^{n+1} B_{\widetilde{k}} \right) \mathcal{N}_{\widetilde{k}}^{\underline{\widetilde{k}}_{\widetilde{f}}} \left|\widetilde{f}\right| \right).
\end{aligned}$$

The water depth $h_{\underline{\widetilde{k}}_{\widetilde{f}}}^{n+1}$ and the velocity $\overline{u}_{\underline{\widetilde{k}}_{\widetilde{f}}}^{n+1}$ are still needed and are obtained by one of the strategies proposed in §4.1. Note that in the case of a imposed discharge in subcritical regime, the water depth $h_{\underline{\widetilde{k}}_{\widetilde{f}}}^{n+1}$ can not be estimated because it depends non-linearly on the velocity $\overline{u}_{\widetilde{k}}^{n+1}$ and an iterative process is needed. In practice, we approach the velocity in the ghost cell by $\frac{\int_{\widetilde{f}} \mathcal{Q}\left(t^{n+1},s\right) \mathrm{d}s}{h_{\underline{\widetilde{k}}_{\widetilde{f}}}^{n}}$, with $\mathcal{Q}\left(t,s\right)$ is the imposed discharged at the bound, in this case for the dispersion step.

5. Numerical results

The current section is devoted to numerical illustrations and comparisons between the models in one dimension framework with a regular mesh, i.e. for any $k \in \mathbb{T}$, $\delta_k = \delta_x = \frac{|k|}{2}$ with $|k|$ the space between two interfaces. The advection step is computed using the HLL scheme with the hydrostatic reconstruction [9]. Even if this scheme does not satisfy Proposition 3.ii), it is largely used in practice and it seems more relevant to illustrate results with this classical scheme. The gravity acceleration is set to $g = 9.81$ for all the following simulations.

5.1. Solitary waves

It is well-known that the dispersive models (E), (NH) and (GN) has a solitary wave solution in one dimension framework on a flat bottom without

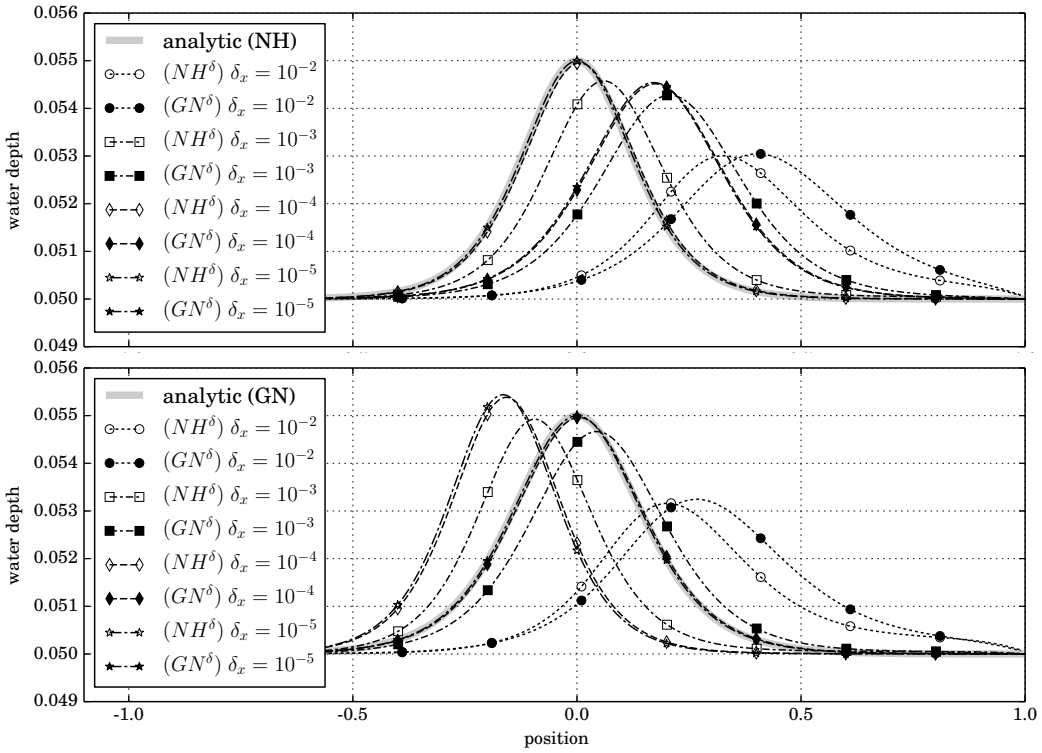

Figure 2: **Solitary waves:** Water depth approximated by (NH^δ) and (GN^δ) at time $t = 50$ initialized by the solitary wave of (NH) (first line) and (GN) (second line).

surface pressure, i.e. $B = P = 0$. Note the solitary wave of each model are not the same. More precisely, in the framework of the solitary waves of (NH) and (GN) read

$$h(t,x) = h^0(x) = H_0 + A\,\mathrm{sech}^2\left(\sqrt{\frac{\gamma^{\mathrm{XX}}A}{A+H_0}}\frac{x}{H_0}\right) \text{ and } \overline{u}(t,x) = \overline{u}^0(x) = \frac{H_0}{h(t,x)}\sqrt{g(H_0+A)} \tag{5.1}$$

with $H_0 > 0$ is the water depth far from the wave and $A > 0$ is the wave elevation. The parameter γ^{XX} depend on the model, i.e. $\gamma^{\mathrm{NH}} = 1$ and $\gamma^{\mathrm{GN}} = {}^3\!/_4$. The vertical velocity and the hydrodynamic pressure can be deduce using the constrains $(NH.\mathrm{b})$ or $(GN.\mathrm{b})$.

In the current section, the solution of the models with the different solitary waves is compared. More precisely we set the parameters

$$H_0 = 5\cdot 10^{-2} \qquad \text{and} \qquad A = 5\cdot 10^{-3}.$$

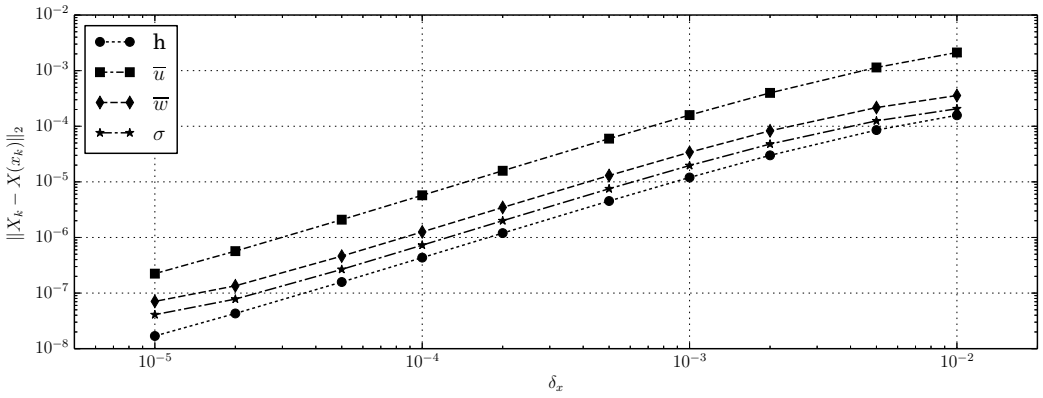

Figure 3: **Solitary waves:** L^2-norm of the difference between the numerical approximation (GN^{δ}) and the analytical solution (5.1) with $\gamma^{\text{XX}} = {}^{3}/_{4}$ as function of the space step at time $t = 50$.

Obviously, the characteristic ratio ${}^{A}/_{H_0}$ of real waves is smaller but this parameters is used to easily observe the differences between the solitary waves. The computational domain is set to $[-1, 1]$. At the left boundary, the discharged is imposed and set to $h\,(t,-1)\,\overline{u}\,(t,-1) = h^0\,(-1)\,\overline{u}^0\,(-1)$ where at the right the water depth is imposed and set to $h\,(t,1) = h^0\,(1)$, see §4.

In Figure 2, the solution of the dispersive models (NH) and (GN) initialized with the solitary wave (5.1) with $\gamma^{\text{XX}} = 1$ (first line) and $\gamma^{\text{XX}} = {}^{3}/_{4}$ (second line) is plotted at time $t = 50$ for some space steps. For small enough space step, the solitary wave of each model is well preserved by the scheme corresponding to the model. The convergence rate, about 1.5, of (GN^{δ}) is illustrated in Figure 3. The same result is observed with (NH^{δ}). The supraconvergence come from the fact that the hyperbolic step (first order) is significantly less important that the dispersive step (expected second order) for this test case. Obviously, the solitary wave is not exactly preserved and a perspective of this work can be to design a scheme able to exactly preserve the solitary wave in its framework, i.e. a well-balanced scheme for the steady solitary waves. This point is discuss in the final conclusion.

5.2. Water drop

The following test case is devoted to the parametric analysis of the aspect ratio. More precisely, (SW) is known as to be a good approximation of

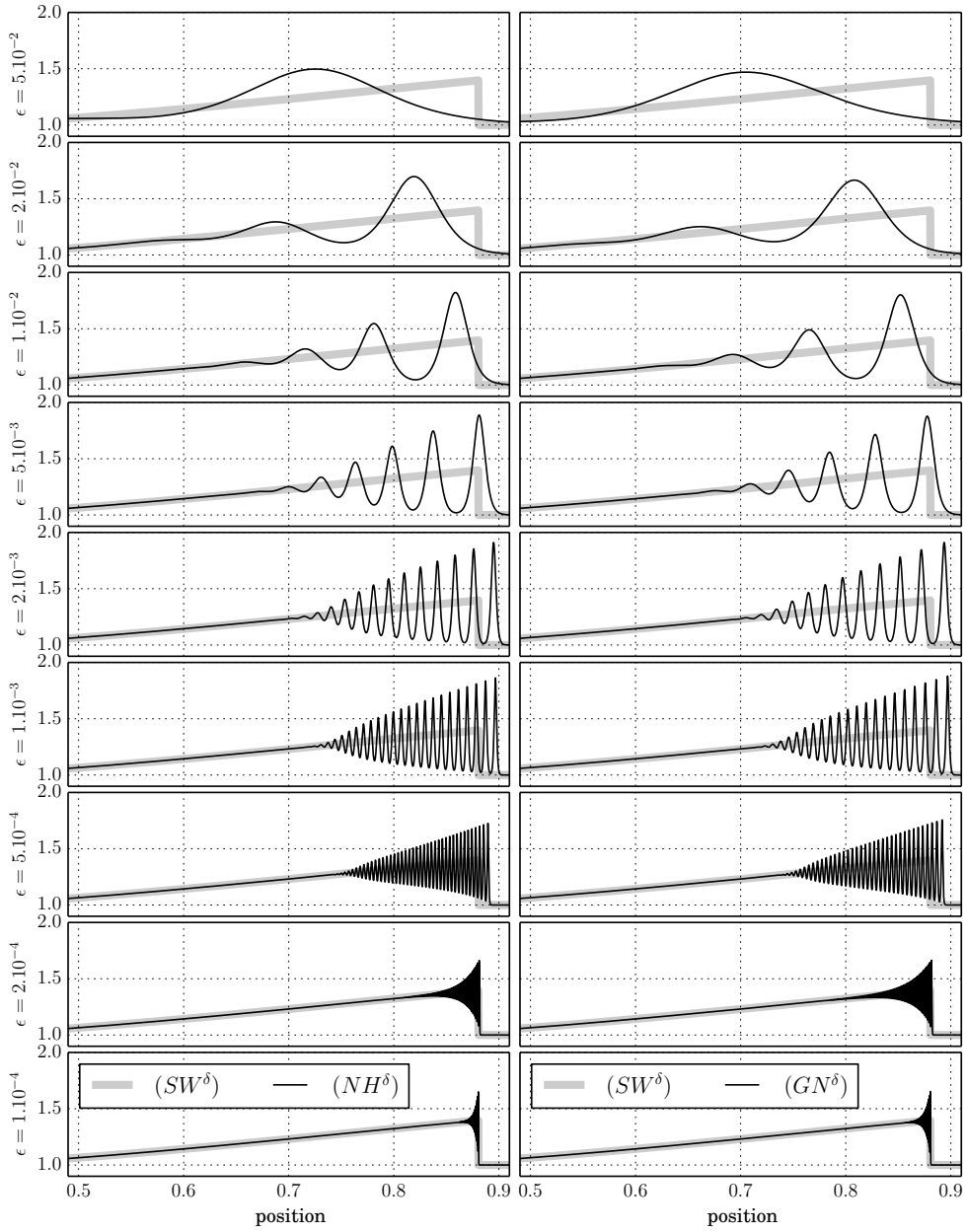

Figure 4: **Water drop:** Rescaled water depth h/ε approximated at the rescaled time $\sqrt{g\varepsilon}t = 0.6$ by (NH^δ) (left column) and (GN^δ) (right column) for several aspect ratio.

(E) when the aspect ratio ε, defined by the ratio between the characteristic

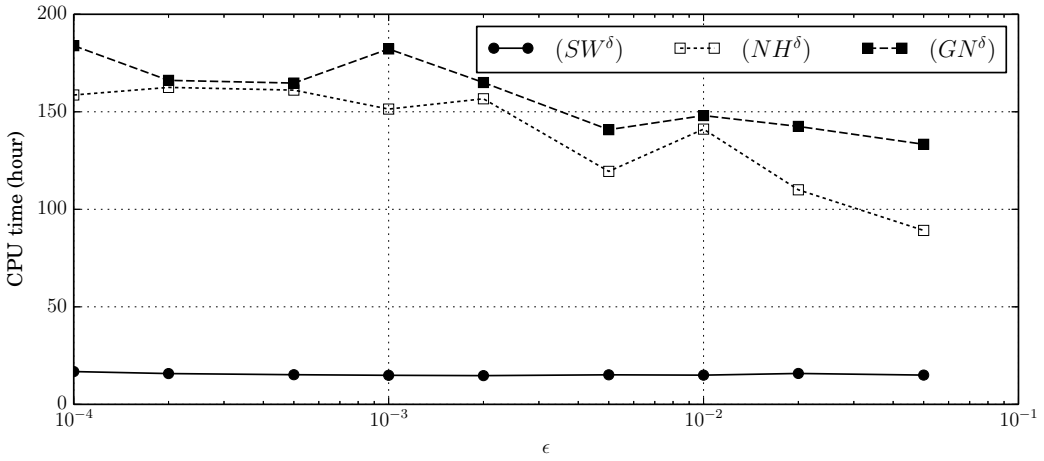

Figure 5: **Water drop:** CPU time of the hierarchy of models to reach the rescaled time $\sqrt{g\bar{\varepsilon}}t = 0.6$ for several aspect ratio.

vertical length and the characteristic horizontal length, is small enough. We propose to compare the dispersive model (NH) and (GN) to (SW) with respect to ε. To do so, the water drop test case seems a good framework.

Let us describe the case precisely. The computational domain is set to $[0, 1]$ and the boundary conditions are walls, see §4. The bottom and the surface pressure vanish at any time $B = P = 0$ and the initial condition is set to

$$h^0(x) = \varepsilon\left(1 + e^{-100x^2}\right) \qquad \text{and} \qquad \overline{u}^0(x) = 0.$$

In Figure 4, the water depth approximated by each models with $\delta_x = 10^{-6}$ is plotted for several aspect ratio. The numerical diffusion probably significantly affect the solution for $\varepsilon \leq 5 \cdot 10^{-4}$. On flat bottom, the solution of the two dispersive models (NH) and (GN) are very similar. The smaller ε is, the higher the oscillation after the front of the wave is with higher frequency. That why the convergence is hard to obtain for very small ε since the frequency of the oscillation is very high. The frequency is slightly higher for (NH) than (GN) even if the shape of the convexe hull is the same, i.e. linear with almost the same slope. It seems clear that (NH^{δ}) and (GN^{δ}) does not converge pointwise. However, the solutions seems converge in L^2-norm.

In Figure 5, the CPU time for each simulations in given. The two dispersive models are computed with almost the same CPU time. The slightly larger CPU time of (GN^{δ}) can be explain by the advection of the standard

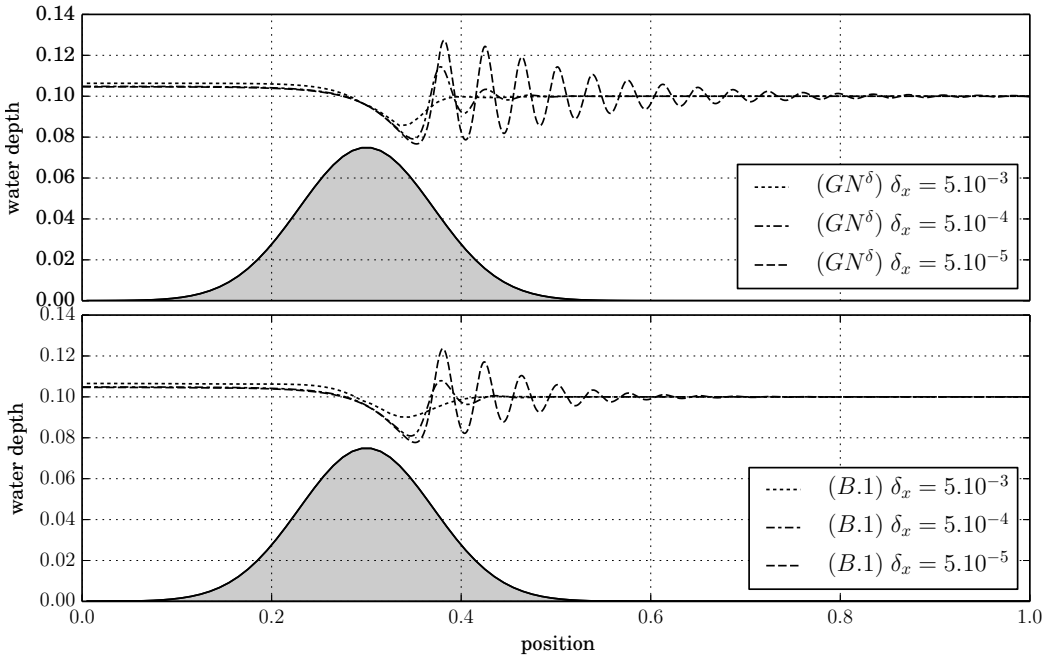

Figure 6: **Undular jump:** Water level approximated by (GN^δ) (first line) and (Appendix B.1) (second line).

deviation. In addition, the CPU time of dispersive models is decreasing with ε while the CPU time of (SW^δ) is almost constant. It can be explained by the oscillations of the dispersive models also visible in the horizontal velocity which affect the time step through the CFL condition (3.2).

5.3. Undular jump

In one dimensional framework, a very classical test case of (SW) is the steady flow with transcritical regime [13]. This analytical solution is based on the energy conservation property, i.e. Proposition 2.ii). More precisely, the energy conservation leads imply for steady flow that the hydraulic head, defined the ratio between the energy flux and the mass flux, i.e.

$$\mathcal{Q} := h\overline{u} \qquad \text{and} \qquad K^{\text{SW}} := \frac{\overline{\mathcal{G}}^h + \overline{\mathcal{G}}^{\overline{u}}}{\mathcal{Q}} = \phi + gh + \frac{|\overline{u}|^2}{2}$$

are piecewise constant. Assuming the hydraulic head at one point, the water depth can be estimated solving a third order polynomial as long as the

solution is continuous. At the discontinuities, the jump should satisfy the Rankine-Hugoniot relations see [13] for details.

Using the same arguments, the hydraulic head of the dispersive models (NH) and (GN) respectively given by

$$K^{\text{NH}} := \frac{\overline{\mathcal{G}}^{h} + \overline{\mathcal{G}}^{\overline{u}} + \overline{\mathcal{G}}^{\overline{w}} + \overline{\mathcal{G}}^{q_B}}{\mathcal{Q}} = \phi + gh + \frac{|\overline{u}|^2}{2} + \frac{|\overline{w}|^2}{2} + \frac{q_B}{2}$$

$$\text{and} \quad K^{\text{GN}} := \frac{\overline{\mathcal{G}}^{h} + \overline{\mathcal{G}}^{\overline{u}} + \overline{\mathcal{G}}^{\overline{w}} + \overline{\mathcal{G}}^{\sigma} + \overline{\mathcal{G}}^{\overline{q}}}{\mathcal{Q}} = \phi + gh + \frac{|\overline{u}|^2}{2} + \frac{|\overline{w}|^2}{2} + \frac{|\sigma|^2}{2} + \overline{q}$$

are piecewise constant. Unfortunately, it is not trivial to recover the water depth form the hydraulic head since the velocity and the hydrodynamic pressure depends on the water depth. Moreover, it is clear that several solutions have the same hydraulic head. For example, the solitary wave (5.1) is a steady solution with the same hydraulic head that the constant solution $h = H_0$ and $\overline{u} = \sqrt{g\,(H_0 + A)}$. However, the analysis of the dispersive models show that the solution is continuous for smooth enough bottom, see [26, 23]. It follows that the hydraulic head is constant in the whole domain then we propose to compare the hydraulic head of the computed approximation to the theoretical hydraulic head estimated at the right bound.

Let us describe the test case more precisely. We consider the computational domain $[0, 10]$ with an imposed discharged at the left bound $h\,(0)\,\overline{u}\,(0) = 10^{-2}$ and an imposed water depth at the right bound $h\,(2) = 10^{-1}$, see §4. The bottom and the surface pressure are set to

$$B\,(x) = 7.5 \cdot 10^{-3}\; e^{-100(x-0.3)^2} \qquad \text{and} \qquad P\,(x) = 0.$$

The water level approximated by (GN^{δ}) and (Appendix B.1) (with XX = GN) for some space step is plotted in Figure 6. Similar results are obtained with the scheme (NH^{δ}). Note that the converged solution is hard to obtain. More precisely, the better the resolution is, the higher the oscillations are and further they expand. It seems that the converged solution present periodic oscillations which does not decrease in amplitude. Thus for a fine enough resolution, the right boundary condition (fixed water depth) become inconsistent and more elaborated boundary condition are required [7, 25]. It is why the computation domain is set large enough in our case. In addition, remark that with the same resolution, the numerical diffusion seems

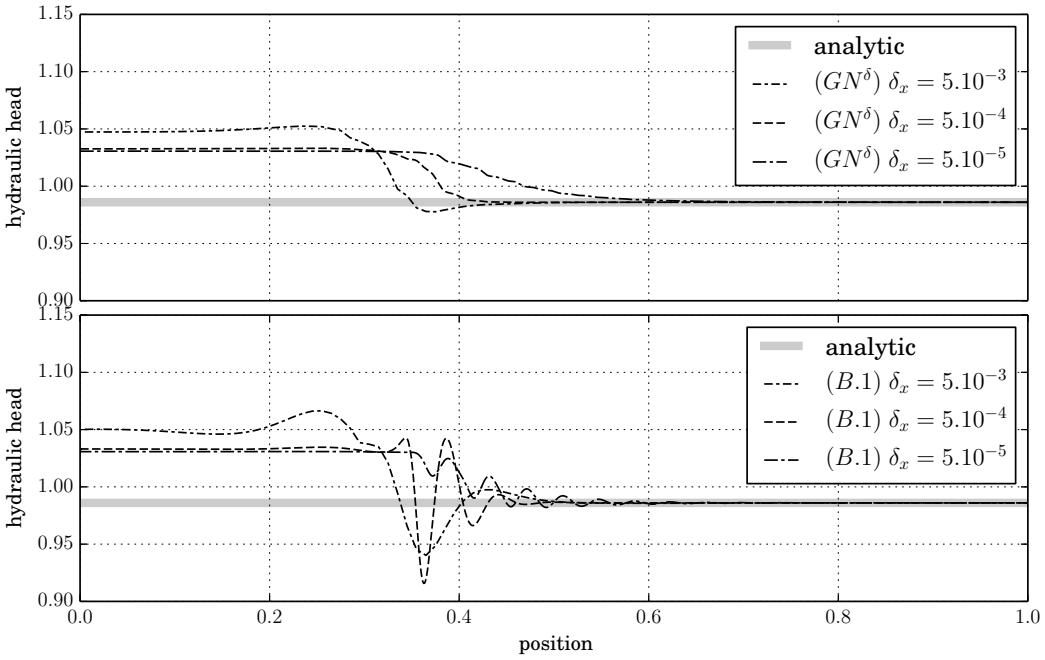

Figure 7: **Undular jump:** Hydraulic head approximated by (GN^δ) (first line) and (Appendix B.1) (second line).

smaller with the entropy-satisfying scheme (GN^δ) than with the compact scheme (Appendix B.1). Anyway, the simulation seems correspond to the undular jump in the Chow's classification, see [40], i.e. for Froude number $1 \leq Fr < 1.7$ whereas the hydraulic jump of (SW) does not correspond to physical observations. We mention that for subcritical flow, i.e. $0 \leq Fr < 1$, any models (SW), (NH) and (GN) lead to similar results which corresponds to observations.

By the way, Even if the analytical solution is not identified, it is clear that the water depth to the left of the bump is higher than it should. More precisely, far enough to the bump, the dispersive effect vanishes and the water depth should be the same than at the right bound since the hydraulic head is constant. In Figure 7, the hydraulic head approximated by the schemes is plotted as well as the analytic hydraulic head. The first observation is that the approximated hydraulic head does not seem converge to the analytic solution and may be link to the hard convergence of the water depth. This drawback probably come from the splitting strategy where at the first step (advection step), the scheme (SW^δ) is used and is consistant with a

solution which dissipate the mechanical energy. A perspective of this work can be to design a scheme able to exactly preserve the the hydraulic head for steady solution. The second observation is that the hydraulic head approximated by (GN^δ) is almost monotonous in contrary to the one approximated by (Appendix B.1). This property is a consequence of Proposition 7.ii). If the hydraulic head is not exactly decreasing in the case of (GN^δ), it is because the HLL scheme with the hydrostatic reconstruction does not satisfy Proposition 3.ii).

5.4. Seawall

To illustrate the robustness of the scheme for moving bottom and at the dry front, the test case of the seawall is presented. Let us describe the case precisely. The computational domain is set to $[0, 10]$ and the boundary conditions are walls, see §4. The surface pressure is neglected $P = 0$ but the bottom is a time and space function given by

$$B(t,x) = \max\left(0, 0.2\,(x-2) + 1.5e^{-10(x-7)^2}, 10\,(x-9)\right) + 10e^{-5(x-2\min(t,1))^2}$$

and the initial condition reads

$$h^0(x) = \begin{cases} \max\left(0, 2 - B(0,x)\right) & \text{if } x \leq 7 \\ 0 & \text{elsewhere} \end{cases} \qquad \text{and} \qquad \overline{u}^0(x) = 0.$$

In Figure 8, the water level approximated by each models with $\delta_x = 10^{-3}$ is plotted at several times. Even if the two dispersive models lead to significantly different results, in particular at dry front, they are qualitatively similar. First, we find that the dispersive models and (SW) respond very differently to the bottom elevation, i.e. $0 \leq t < 1$. In the case of (SW), the water level does not become much higher than the initial condition, i.e. 3m, and a wave is promptly generated. In the case of the dispersive models, the water level become higher, i.e. 4m, and the beginning of the wave is not as clear. Any models is able to pass the seawall but the shape of the water level is different. In the case of (SW), the water level is discontinuous before the seawall and continuous after whereas for the dispersive models the water level is continuous before the seawall and discontinuous at the dry front, at least for a moment. The velocity of the dry front is lower for the dispersive models, in particular for (GN^δ). Note that this result is largely affected by the choice of the velocity in the dry areas. We recall that the proposed solution is based on the dissipation of the mechanical energy, see

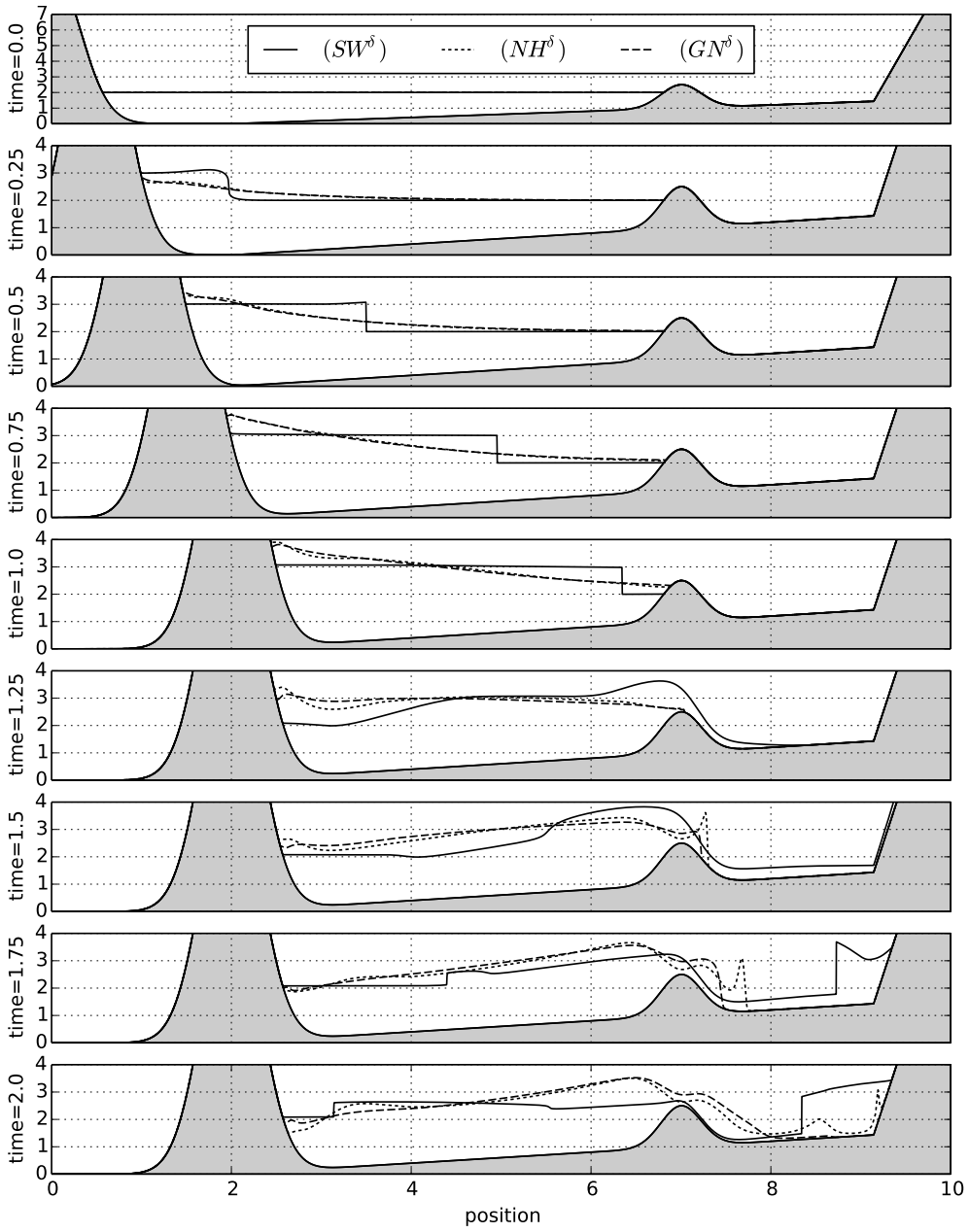

Figure 8: **Seawall:** Water level approximated by the hierarchy of models at several times.

Proposition 5 and Proposition 7. The schemes are able to deal with creation of dry areas or wet areas.

Conclusion

The current paper, the first in a series of two, focuses on the numerical resolution in multidimensional framework of a hierarchy of monolayer dispersive models, such is the Serre-Green-Naghdi model (GN). A particular attention is given to the dissipation of the mechanical energy at the discrete level. To illustrate the accuracy and the robustness of the strategy, several numerical experiments are performed. In particular, the strategy is able to deal with dry areas without particular treatment.

To improve the numerical approximation, two perspectives can be highlighted. First, even if the solitary waves of each models is well recover when the space step goes to zero, it is not exactly preserved, see §5.1. It may be possible to design a scheme that exactly preserves a discretization of the solitary wave in its framework. Secondly, the solution converge very slowly in the case of an undular jump, see §5.3. More precisely, the converge solution should not dissipate the mechanical energy but the numerical experiments seems indicate that even at convergence there is a dissipation even if it is largely smaller than for the shallow water model (SW). In our mind, that two points came from the splitting strategy between the hyperbolic and dispersive parts of the equations and it is clearly not trivial to fix them preserving the efficiency of the method.

The second part of this work ([32]) will be devoted to the layerwise dispersive models see [18]. With these schemes, we expect to illustre the convergence of the layerwise models to solution of the free surface Euler model (E) for smooth enough solution. In addition, we expect to simulate hydraulic jump with higher Froude number, for instead weak jumps, i.e. $1.7 \leq Fr < 2.5$. Accordingly to the Chow's description, this hydraulic jump create a underlying current that could not be described by monolayer models.

Acknowledgements

I would like to thank E. D. Fernandez-Nieto, Y. Penel and J. Sainte-Marie for exchanges and discussions about the models and the different numerical strategies, the Alpines Inria project team members with in particular S. Cayrols, O. Tissot, H. Al Daas for their help with the linear algebra library (Intel® Math Kernel Library) used for this work, and E. Audusse for his kind advises. This work is a part of the research project CNRS-PICS-07480.

References

[1] Aguillon, N., Audusse, E., Godlewski, E. & Parisot, M. (2017) Hyperbolicity of the Layerwise Discretized Hydrostatic Euler equation : the bilayer case. working paper or preprint.

[2] Aissiouene, N., Bristeau, M.-O., Godlewski, E. & Sainte-Marie, J. (2015) A robust and stable numerical scheme for a depth-averaged Euler system. working paper or preprint.

[3] Aissiouene, N., Bristeau, M.-O., Godlewski, E. & Sainte-Marie, J. (2016) A combined finite volume - finite element scheme for a dispersive shallow water system. *Networks and Heterogeneous Media (NHM)*.

[4] Audusse, E., Bouchut, F., Bristeau, M.-O., Klein, R. & Perthame, B. (2004) A fast and stable well-balanced scheme with hydrostatic reconstruction for shallow water flows. *SIAM J. Sci. Comput.*, **25**, 2050–2065.

[5] Audusse, E., Bristeau, M.-O., Perthame, B. & Sainte-Marie, J. (2011) A multilayer Saint-Venant system with mass exchanges for shallow water flows. Derivation and numerical validation. *ESAIM: M2AN*, **45**, 169–200.

[6] Audusse, E., Bouchut, F., Bristeau, M.-O. & Sainte-Marie, J. (2015) Kinetic entropy inequality and hydrostatic reconstruction scheme for the Saint-Venant system. Accepted for publication in Math. Comp.

[7] Besse, C., Noble, P. & Sanchez, D. (2017) Discrete transparent boundary conditions for the mixed KDV–BBM equation. *Journal of Computational Physics*, **345**, 484 – 509.

[8] Bonneton, P., Chazel, F., Lannes, D., Marche, F. & Tissier, M. (2011) A splitting approach for the fully nonlinear and weakly dispersive Green–Naghdi model. *Journal of Computational Physics*, **230**, 1479–1498.

[9] Bouchut, F. (2004) *Nonlinear stability of finite volume methods for hyperbolic conservation laws, and well-balanced schemes for sources*. Springer Science & Business Media.

[10] Bristeau, M.-O., Mangeney, A., Sainte-Marie, J. & Seguin, N. (2015) An energy-consistent depth-averaged Euler system: Derivation and properties. *Discrete and Continuous Dynamical Systems - Series B*, **20**, 961–988.

[11] Castro, A. & Lannes, D. (2014) Fully nonlinear long-wave models in the presence of vorticity. *Journal of Fluid Mechanics*, **759**, 642–675.

[12] Castro, M., Gallardo, J. M., López-García, J. A. & Parés, C. (2008) Well-balanced high order extensions of Godunov's method for semilinear balance laws. *SIAM J. Numer. Anal.*, **46**, 1012–1039.

[13] Chanson, H. (1959) *Open-channel hydraulics*. Butterworth-Heinemann.

[14] Chazel, F., Lannes, D. & Marche, F. (2010) Numerical Simulation of Strongly Nonlinear and Dispersive Waves Using a Green–Naghdi Model. *Journal of Scientific Computing*, **48**, 105–116.

[15] Cienfuegos, R., Barthélemy, E. & Bonneton, P. (2006) A fourth-order compact finite volume scheme for fully nonlinear and weakly dispersive Boussinesq-type equations. Part I: model development and analysis. *International Journal for Numerical Methods in Fluids*, **51**, 1217–1253.

[16] Couderc, F., Duran, A. & Vila, J.-P. (2017) An explicit asymptotic preserving low froude scheme for the multilayer shallow water model with density stratification. *Journal of Computational Physics*, **343**, 235 – 270.

[17] de Saint-Venant, A.-J.-C. B. (1871) Théorie du mouvement non permanent des eaux, avec application aux crues des rivières et à l'introduction des marées dans leurs lits. *C.R. Acad. Sci. Paris*, **73**, 147–154.

[18] Fernandez-Nieto, E. D., Parisot, M., Penel, Y. & Sainte-Marie, J. (2016) Layer-averaged approximation of Euler equations for free surface flows with a non-hydrostatic pressure. working paper or preprint.

[19] Gerbeau, J.-F. & Perthame, B. (2001) Derivation of viscous saint-venant system for laminar shallow water; numerical validation. *Discrete and Continuous Dynamical Systems - Series B*, **1**, 89–102.

[20] Godlewski, E. & Raviart, P.-A. (1996) *Numerical approximation of hyperbolic systems of conservation laws*. Applied Mathematical Sciences, vol. 118. Springer-Verlag, New York, pp. viii+509.

[21] Godunov, S. K. (1959) A difference method for numerical calculation of discontinuous solutions of the equations of hydrodynamics. *Mat. Sb. (N.S.)*, **47(89)**, 271–306.

[22] Green, A. E. & Naghdi, P. M. (1976) A derivation of equations for wave propagation in water of variable depth. *Journal of Fluid Mechanics*, **78**, 237–246.

[23] Israwi, S. (2011) Large time existence for 1D Green-Naghdi equations. *Nonlinear Analysis: Theory, Methods & Applications*, **74**, 81–93.

[24] Jin, S. & Wen, X. (2005) Two interface-type numerical methods for computing hyperbolic systems with geometrical source terms having concentrations. *SIAM J. Sci. Comput.*, **26**, 2079–2101 (electronic).

[25] Kazakova, M. & Noble, P. (2017) Discrete transparent boundary conditions for the linearised Green-Naghdi system of equations. working paper or preprint.

[26] Lannes, D. & Alvarez-Samaniego, B. (2008) A Nash-Moser theorem for singular evolution equations. Application to the Serre and Green-Naghdi equations. *Indiana Univ. Math. J.*, **57**, 97–132.

[27] Lannes, D. & Bonneton, P. (2009) Derivation of asymptotic two-dimensional time-dependent equations for surface water wave propagation. *Physics of Fluids*, **21**.

[28] Lannes, D. & Marche, F. (2015) A new class of fully nonlinear and weakly dispersive Green–Naghdi models for efficient 2D simulations. *Journal of Computational Physics*, **282**, 238–268.

[29] Le Métayer, O., Gavrilyuk, S. & Hank, S. (2010) A numerical scheme for the Green–Naghdi model. *Journal of Computational Physics*, **229**, 2034 – 2045.

[30] LeVeque, R. J. (2002) *Finite volume methods for hyperbolic problems*, vol. 31. Cambridge university press.

[31] Noelle, S., Xing, Y. & Shu, C.-W. (2007) High-order well-balanced finite volume WENO schemes for shallow water equation with moving water. *J. Comput. Phys.*, **226**, 29–58.

[32] Parisot, M. (2017) Entropy-satisfying scheme for a hierarchy of dispersive reduced models of free surface flow, Part II. working paper or preprint.

[33] Parisot, M. & Vila, J.-P. (2016) Centered-potential regularization for the advection upstream splitting method. *SIAM Journal on Numerical Analysis*, **54**, 3083–3104.

[34] Peregrine, D. H. (1967) Long waves on a beach. *Journal of Fluid Mechanics*, **27**, 815–827.

[35] Perthame, B. & Simeoni, C. (2001) A kinetic scheme for the saint-venant system with a source term. *Calcolo*, **38**, 201–231.

[36] Richard, G. L. & Gavrilyuk, S. L. (2012) A new model of roll waves: comparison with brock's experiments. *Journal of Fluid Mechanics*, **698**, 374–405.

[37] Richard, G. L. & Gavrilyuk, S. L. (2013) The classical hydraulic jump in a model of shear shallow-water flows. *Journal of Fluid Mechanics*, **725**, 492–521.

[38] Serre, F. (1953) Contribution à l'étude des écoulements permanents et variables dans les canaux. *La Houille Blanche*, 830–872.

[39] Suliciu, I. (1990) On modelling phase transitions by means of rate-type constitutive equations. shock wave structure. *International Journal of Engineering Science*, **28**, 829–841.

[40] Te Chow, V. (1959) *Open-channel hydraulics*. McGraw-Hill civil engineering series. McGraw-Hill.

[41] Teshukov, V. M. (2007) Gas-dynamic analogy for vortex free-boundary flows. *Journal of Applied Mechanics and Technical Physics*, **48**, 303–309.

[42] Toro, E. F. (2013) *Riemann solvers and numerical methods for fluid dynamics: a practical introduction*. Springer Science & Business Media.

Appendix A. Formal derivation of (*GN*)

In the current section, the main steps of a formal derivation of the Serre-Green-Naghdi model leading to the formulation (*GN*) are remind. For more details, we refer to [18].

Proposition 8. *Let $\varepsilon > 0$ be a small enough parameter. Assume that the solution of the Euler model (E) satisfies the following scaling*

$$\forall\,(t,x,z) \in \mathbb{R}_+ \times \mathbb{R}^d \times \mathbb{R} \qquad u\,(t,x,z) - \langle u\rangle\,(t,x) = O\,(\varepsilon) \tag{A.1}$$

with $\langle\psi\rangle = \frac{1}{\eta - B}\int_B^\eta \psi\,\mathrm{d}z$. Assume in addition that the topography, the water depth and the pressure are regular enough. Then the vertical averaged model (GN) with the initial condition

$$h\,(0,x) = \eta^0\,(x) - B\,(0,x)\,, \qquad \overline{u}\,(0,x) = \left\langle u^0\right\rangle$$

results from an approximation of the Euler model (E). More precisely, the modelling error reads

$$\begin{gathered}\eta - B - h = O\,(\varepsilon)\,, \quad u - \overline{u} = O\,(\varepsilon)\,, \quad w - \left(\overline{w} + 2\sqrt{3}\frac{z - B - \frac{h}{2}}{h}\sigma\right) = O\,(\varepsilon)\,,\\ q - \left(\frac{B + h - z}{h}q_B - 3\frac{(z - B)\,(B + h - z)}{h^2}\,(q_B - 2\overline{q})\right) = O\,(\varepsilon)\,.\end{gathered} \tag{A.2}$$

Proof. First of all, the mass conservation can be obtained by integration along the vertical axis of the divergence free constrain between the bottom B and the free surface η. Using the no-penetration at bottom and the kinematic condition at free surface, it reads

$$\partial_t\,(\eta - B) + \nabla\cdot((\eta - B)\,\langle u\rangle) = 0.$$

The vertical-averaged horizontal velocity is obtained by integrating the horizontal momentum equation of (*E*). More precisely, it reads

$$\partial_t\,((\eta - B)\,\langle u\rangle) + \nabla\cdot((\eta - B)\,\langle u\otimes u\rangle + (\eta - B)\,\langle q\rangle\,\mathbf{I}_d) = -\,(\eta - B)\,\nabla\,(P + g\eta)\,.$$

Similarly, the vertical-averaged vertical velocity reads

$$\partial_t \left((\eta - B) \langle w \rangle \right) + \nabla \cdot \left((\eta - B) \langle wu \rangle \right) = q_B.$$

Using the hypothesis on the velocity profile (A.1), the non-linear integral terms are approached as

$$\langle u \otimes u \rangle = \langle u \rangle \otimes \langle u \rangle + O\left(\varepsilon^2\right) \qquad \text{and} \qquad \langle wu \rangle = \langle w \rangle \langle u \rangle + O\left(\varepsilon\right).$$

By integrating the divergence free (first equation of (E)) between B and an arbitrary $z \in [B, \eta]$ the vertical velocity mainly scales as a linear function of the vertical coordinate. More precisely, it reads $w = \langle w \rangle + 2\sqrt{3} \frac{z - \frac{\eta+B}{2}}{\eta - B} \langle \sigma \rangle + O\left(\varepsilon\right)$ with

$$\langle w \rangle = \partial_t \left(\frac{\eta + B}{2} \right) + \langle \overline{u} \rangle \cdot \nabla \left(\frac{\eta + B}{2} \right) \quad \text{and} \quad \langle \sigma \rangle = \frac{\partial_t \left(\eta - B \right) + \overline{u} \cdot \nabla \left(\eta - B \right)}{2\sqrt{3}}.$$

The new variable $\langle \sigma \rangle$ is the oriented standard deviation in the sens that it satisfies $\langle \sigma \rangle^2 = \left\langle \left(w - \langle w \rangle \right)^2 \right\rangle$. Similarly, by integration of the vertical velocity equation (third equation of (E)) between B and an arbitrary $z \in [B, \eta]$, the hydrodynamic pressure mainly scales as a quadratic function of the vertical coordinate. Thus, since the hydrodynamic pressure vanishes at free surface $q_{z=\eta} = 0$, it can be defined by its value at the bottom $q_{|_{z=B}}$ and its vertical-averaged value $\langle q \rangle$ such that the hydrodynamic pressure reads the reconstruction defined by (A.2).

The last step of the derivation is the establishment of the evolution equation on the standard deviation. Applying the vertical derivative on the third equation of (E), it yields to

$$\partial_t \left(\partial_z w \right) + u \cdot \nabla \left(\partial_z w \right) + \left(\partial_z w \right)^2 = -\partial_z^2 q + O\left(\varepsilon\right).$$

Since the hydrodynamic pressure is quadratic, the right-hand side reads $\partial_z^2 q = \frac{6}{(\eta - B)^2} \left(q_{|_{z=B}} - 2 \langle q \rangle \right)$. Note that the equation on the perturbation of the vertical velocity can be used instead of the last equation of (GN). However, to obtain a more classical form, we remark that

$$\partial_t \left((\eta - B) \langle \sigma \rangle \right) + \nabla \cdot \left((\eta - B) \langle \sigma \rangle \langle u \rangle \right) = -\frac{(\eta - B)^2}{2\sqrt{3}} \left(\partial_t \left(\partial_z w \right) + u \cdot \nabla \left(\partial_z w \right) + \left(\partial_z w \right)^2 \right) + O\left(\varepsilon\right).$$

We conclude that the model (GN) is an approximation of the Euler model (E) where h, $\overline{u}$, $\overline{w}$, σ, $\overline{q}$ and q_B are respectively the approximation at order

ε of the water depth $\eta - B$, the vertical-averaged horizontal velocity $\langle u \rangle$, the vertical-averaged vertical velocity $\langle w \rangle$, the oriented standard deviation $\langle \sigma \rangle$, the vertical-averaged hydrodynamic pressure $\langle q \rangle$ and the pressure at bottom $q_{|z=B}$. □

Eventually, (NH) can be obtained from (GN) assuming that σ is negligible. More precisely since the left-hand side of is negligible the fourth equation of (GN), the vertical-averaged hydrodynamic pressure reads $\overline{q}^{\text{NH}} = \frac{q_B^{\text{NH}}}{2}$ and it yields (NH).

Appendix B. Dispersion step with a compact operator

The discrete operator of the dispersion step (NH^{δ}.b) or (GN^{δ}.b) is a 5-point stencil in one dimension. This large stencil limit the performance of the scheme and leads to complexe boundary conditions. One can remark that the scheme is a discretization of a reaction-advection-diffusion equation. A strategy that can be use to reduce the stencil of the scheme is to establish the reaction-advection-diffusion equation mimicking the step realized to obtain the scheme (NH^{δ}.b) or (GN^{δ}.b) at the continuous framework, then use a more compact discretization. The resulting scheme reads

$$\begin{aligned}
&\alpha_k^{\text{XX}} \overline{u}_k^{n+1} + \nabla_k^{\delta} \left(\mu^{\text{XX}} \cdot \overline{u}^{n+1} \right) - \mu_k^{\text{XX}} \nabla_k^{\delta} \cdot \overline{u}^{n+1} \\
&\quad - \frac{1}{|k|} \sum_{f \in \mathbb{F}_k} \left(\frac{\kappa_k^{\text{XX}}}{\delta_k} + \frac{\kappa_{\underline{k}_f}^{\text{XX}}}{\delta_{\underline{k}_f}} \right) \frac{\overline{u}_{\underline{k}_f}^{n+1} - \overline{u}_k^{n+1}}{2} \cdot \mathcal{N}_k^{\underline{k}_f} \mathcal{N}_k^{\underline{k}_f} |f| = \beta_k^{\text{XX}}
\end{aligned} \tag{Appendix B.1}$$

with the parameters α_k^{XX}, μ_k^{XX}, κ_k^{XX} and β_k^{XX} ($\text{XX} \in \{\text{NH}, \text{GN}\}$) defined in ($NH^{\delta}$.b) or ($GN^{\delta}$.b). The yielding scheme (Appendix B.1) is more compact, i.e. 3-point stencil in one dimension. In one dimension, the scheme can be even more simpler by developing the first order derivative before the discretization and leads to a reaction-diffusion equation. However, the compact scheme (Appendix B.1) does not ensure the mechanical energy dissipation and in less accurate than (NH^{δ}.b) or (GN^{δ}.b) in practice.